NBSIR 80-2010

Analysis of Construction Conditions Affecting the Structural Response of the Cooling Tower at Willow Island, West Virginia

H. S. Lew and S. G. Fattal

Structures and Materials Division
Center for Building Technology
National Engineering Laboratory
National Bureau of Standards
U.S. Department of Commerce
Washington, D.C. 20234

July 1980

NBS-114A (REV. 9-78)

U.S. DEPT. OF COMM. BIBLIOGRAPHIC DATA SHEET	1. PUBLICATION OR REPORT NO. NBSIR 80-2010	2. Gov't Accession No.	3. Recipient's Accession No. PB80 22 26

4. TITLE AND SUBTITLE Analysis of Construction Conditions Affecting the Structural Response of the Cooling Tower at Willow Island, West Virginia	5. Publication Date July 1980
	6. Performing Organization Code

7. AUTHOR(S) H. S. Lew and S. G. Fattal	8. Performing Organ. Report No.

9. PERFORMING ORGANIZATION NAME AND ADDRESS NATIONAL BUREAU OF STANDARDS DEPARTMENT OF COMMERCE WASHINGTON, DC 20234	10. Project/Task/Work Unit No.
	11. Contract/Grant No.

12. SPONSORING ORGANIZATION NAME AND COMPLETE ADDRESS (Street, City, State, ZIP) Occupational Safety and Health Administration Department of Labor Washington, D.C. 20001	13. Type of Report & Period Covered
	14. Sponsoring Agency Code

15. SUPPLEMENTARY NOTES

☐ Document describes a computer program; SF-185, FIPS Software Summary, is attached.

16. ABSTRACT (A 200-word or less factual summary of most significant information. If document includes a significant bibliography or literature survey, mention it here.)

The initial investigation of the Willow Island cooling tower collapse (NBSIR 78-1578) established that the most probable cause of the collapse was the imposition of construction loads on the tower before the concrete had gained adequate strength. The analysis presented herein responds to questions outside the scope of that investigation which considered only actual conditions existing at the time of the collapse. The present investigation shows that failure would initiate in lift 28 if the concrete strength in that lift is 1000 psi (6.9 MPa) or less, and to maintain a safety factor of 2.0, the concrete strength in that lift should be 4000 psi (27.6 MPa). This study also reveals that even if an additional bolt had been introduced between each exterior jumpform beam and the tower, the stresses would not have been relieved enough to prevent failure of lift 28. Finally, it is shown, that if the ground anchor point of the static line had been kept at the location occupied just prior to its last move to a location near the center of the tower, the stresses in the shell due to construction loads would have been relieved to the extent that failure of lift 28 would probably not have occurred.

17. KEY WORDS (six to twelve entries; alphabetical order; capitalize only the first letter of the first key word unless a proper name; separated by semicolons)

Collapse; concrete; concrete strength; construction; construction loads; cooling tower; dynamic effects; failure; failure investigation; hoisting loads; hyperbolic shell

| 18. AVAILABILITY [X] Unlimited	19. SECURITY CLASS (THIS REPORT)	21. NO. OF PRINTED PAGES
☐ For Official Distribution. Do Not Release to NTIS	UNCLASSIFIED	49
☐ Order From Sup. of Doc., U.S. Government Printing Office, Washington, DC 20402, SD Stock No. SN003-003-	20. SECURITY CLASS (THIS PAGE)	22. Price
[X] Order From National Technical Information Service (NTIS), Springfield, VA. 22161	UNCLASSIFIED	$6.00

USCOMM-DC

Figure 5.3   Section capacity of concrete for f'$_c$ = 220 psi
(1.52 MPa) vs. hoop stress resultants at locations
C and D in the shell

NBSIR 80-2010

ANALYSIS OF CONSTRUCTION CONDITIONS AFFECTING THE STRUCTURAL RESPONSE OF THE COOLING TOWER AT WILLOW ISLAND, West Virginia

H. S. Lew and S. G. Fattal

Structures and Materials Division
Center for Building Technology
National Engineering Laboratory
National Bureau of Standards
U.S. Department of Commerce
Washington, D.C. 20234

July 1980

ANALYSIS OF CONSTRUCTION CONDITIONS AFFECTING
THE STRUCTURAL RESPONSE OF THE COOLING TOWER AT
WILLOW ISLAND, WEST VIRGINIA

by

H. S. Lew and S. G. Fattal

ABSTRACT

The initial investigation of the Willow Island cooling tower collapse
(NBSIR 78-1578) established that the most probable cause of the collapse
was the imposition of construction loads on the tower before the concrete
had gained adequate strength. The analysis presented herein responds
to questions outside the scope of that investigation which considered
only actual conditions existing at the time of the collapse. The pre-
sent investigation shows that failure would initiate in lift 28 if the
concrete strength in that lift is 1000 psi (6.9 MPa) or less, and to
maintain a safety factor of 2.0, the concrete strength in that lift
should be 4000 psi (27.6 MPa). This study also reveals that even if an
additional bolt had been introduced between each exterior jumpform beam
and the tower, the stresses would not have been relieved enough to pre-
vent failure of lift 28. Finally, it is shown, that if the ground
anchor point of the static line had been kept at the location occupied
just prior to its last move to a location near the center of the tower,
the stresses in the shell due to construction loads would have been
relieved to the extent that failure of lift 28 would probably not have
occurred.

Key Words: Collapse; concrete; concrete strength; construction; con-
            struction loads; cooling tower; dynamic effects; failure;
            failure investigation; hoisting loads; hyperbolic shell.

Table of Contents

1. INTRODUCTION

1.1 Background

On April 27, 1978, one of two natural-draft hyperbolic concrete cooling towers at Willow Island, West Virginia, collapsed during construction, bringing down with it a four-level scaffold system attached to the collapsed portion of the shell and killing all 51 workers who were on the scaffold. The National Bureau of Standards (NBS) investigated the collapse on behalf of the Occupational Safety and Health Administration (OSHA) to determine the most probable cause of the collapse.

The NBS investigation, which has been documented in detail in a preceding report [1]*, indicated that the most probable cause of the collapse was the imposition of construction loads on a portion of the shell before the concrete in that portion had gained adequate strength to support these loads. The study also indicated that major components of the hoisting, scaffolding and formwork system did not fail prior to the collapse, and ruled out the possibility of the concrete bucket having impacted cathead no. 4 and thereby initiating the collapse.

Figure 1.1 is a schematic illustration of the overall shape the tower would have assumed upon completion. The concrete was being cast at the rate of one 5-ft (1.5-m) high lift per day. On the day of the collapse, the casting of concrete had just begun at an elevation of 166 ft (51m) above grade level as indicated in Figure 1.1.

Figure 1.2 illustrates the construction scheme used at the Willow Island site. A four-level scaffolding system around both the inside and outside periphery of the shell, the six equally spaced catheads, and the hoisting loads transmitted through the catheads, were supported by the completed top portion of the shell, mostly by lift 28, cast the day before the collapse occurred. It was established that the collapse did initiate in lift 28 in the region where cathead no. 4 was located. This occurred when a bucketful of concrete being delivered to cathead no. 4 was about midway to the top and no other hoisting was being carried out. The chain of events reconstructed from witness statements was as follows. After the initial rupture, cathead no. 4 slowly tilted toward the inside of the tower dragging with it lift 28 and the scaffolding attached to it. Lift 28 continued to peel off with failure radiating circumferentially from cathead no. 4 in two opposite directions. The entire lift 28, together with the scaffolding, formwork, the six catheads and 51 workers plummeted to the ground on the inside periphery of the tower.

---

* Numbers in brackets refer to the references listed at the end of this report.

1.2 Scope and Approach

Subsequent to the initial investigation, a number of questions were raised that were not within of the scope of that investigation. This study addresses three major questions that were raised by OSHA.

One of the questions relates to the minimum concrete strength requirement to resist the expected construction loads. Specifically, what should have been the strength of the partially cured concrete in lift 28 so that the shell would have sufficient capacity to resist the applied construction loads with a margin of safety consistent with established engineering practice?

In this study, the problem is analyzed from the point of view of the construction system designer, which takes into account possible amplification of construction loads due to dynamic effects, particularly those inherent in the hoisting system used. The evaluation of dynamic amplification of hoisting loads, however, depends in a major way upon the manner with which the hoisting system was being operated at the time of the collapse. Because of insufficient information, such dynamic effects could not be assessed in the first study. However, this ommission did not alter the conclusions of that study because the capacity of the concrete was exceeded even without considering dynamic effects.

Estimation of dynamic forces is a necessary and integral part in the design of the construction scheme used, because the required margins of safety have to be maintained, even against peak dynamic load fluctuations. It should be noted again that while dynamic effects cannot be evaluated precisely, it is possible to examine upper- and lower-bound conditions within which hoisting load fluctuations can be bracketed. These bounds are established by taking into consideration various possible modes of operation of the hoisting system.

The two remaining questions deal with certain aspects of construction practices that are different from those present at the time of the collapse and thus were not included within the scope of the first report. One of the questions pertains to the lowest line of bolts that would have provided an additional point of connection between each exterior jumpform beam and the shell near the base of lift 27. These bolts were not in place at the time of the collapse, and it is of interest to examine whether their presence would have prevented the initiation of failure in lift 28. The question is addressed by evaluating the stresses at the critical locations in the shell with the lowest bolts in place, and comparing these stresses with the resistance of the shell in lift 28.

The purpose of the last question is to determine whether the collapse could have been prevented if the anchorage point at the lower end of the static line were kept at the previous location. The anchorage point was moved to a location nearer to the center of the tower (where it was at the time of the collapse) after lift 25 was cast. The problem is

2

solved by establishing the spatial configuration of the static line using the specified previous support location and an analytical procedure which closely follows the steps used in the initial investigation [1].

2. DYNAMIC ANALYSIS OF HOISTING LOADS

2.1 Introduction

Figure 2.1, reproduced from ref. 1, shows the hoisting system used for delivery of concrete to the top of the tower at cathead no. 4 at the time of the collape. The lifting of concrete is controlled by the hoist drum operator stationed at U. From the drum, the hoist line proceeds toward and around an interior sheave at T and an exterior sheave at Q, up and around the two sheaves suspended from the cathead beam, and, before hoisting commences, down to a concrete hopper at B near loading platform A at the center of the tower. The static line BG suspended from the cathead beam and anchored to the ground functions as a guide to the hoistline during delivery of materials. Point B_1 represents the anchor point of the static line before the last move to B (see sec. 5).

The initial investigation of the hoisting system documented in ref. 1 was based on a static analysis of the forces in the hoisting cable and the static line as a function of the position of the concrete bucket at various intervals along the static line. The analysis described herein computes forces in the hoisting cable and the static line during a lifting cycle. It takes into consideration the dynamic response of the system based on various assumptions on operating procedures of the drum hoist. Section 2.2 cites all the assumptions made in the analysis and discusses their effects on results. Section 2.3 describes the procedure used in a computer program written specifically for the dynamic analysis of hoisting forces. Section 2.4 presents the two limiting load cases considered in the analysis by assuming the hoistline at takeoff to be initially taut and initially slack, respectively. The results of the analysis and conclusions drawn are discussed in section 2.5.

2.2 Assumptions

The specific assumptions made in the dynamic analysis of hoisting forces and the effects of these assumptions on results are as follows:

1. The hoisting system is idealized as an undamped, linear elastic system. All materials remain in the elastic range, and cable deformations are small. Since the concrete bucket moves about 200 feet (61 m) during a hoisting cycle, the rigid body displacements of the cable are not small, and therefore are considered in the analysis. Principal sources of energy dissipation in the hoisting system are friction damping between the cable strands, and between the sheaves and their supports. Such energy dissipation could probably be idealized using equivalent viscous damping of one or two percent of critical, which will have a negligile effect on the results.

3

2. The transverse movement of the concrete bucket in space is neglected; i.e., the bucket is assumed to move vertically from the ground to the cathead beam. The justifications for this simplification are discussed below.

The actual path of the bucket is curvilinear as shown in figure 2.2. The mass of the bucket moving along this path exerts a centripetal force which increases the tension in the static line by a negligible amount, as pointed out in section 6.8 of reference 1. It is also noted (section 6.7, reference 1) that the speed of the bucket was estimated at 10 fps (3.0 m/s) and that maximum hoisting loads computed by static analysis occurred when the bucket was about 120 ft (36.6 m) below the cathead beam. This places the bucket within the middle third region of the span where the path is relatively flat and approximately parallel to the chord to the static line. For example, within a 15-ft (4.6-m) length of the path between points 113-132 ft (34.5-39.0 m) below the cathead beam (a distance traversed in 1.5 sec), the bucket rotates about the cathead sheave (figure 2.2) through an angle of 0.01 radians. The corresponding centripetal force in the hoistline is about 0.3 lb (1.3 N), which is insignificant. Therefore, the effect of the angular velocity of the bucket on the forces in both the static and hoisting cables was neglected and the bucket was assumed to travel in a straight line from the ground to the cathead beam.

The additional error introduced by neglecting the slope of the static line and assuming the bucket to move vertically up is small as indicated by the following. Neglecting the self-weight of the hoisting cable which is small, the static tension in the hoistline if the bucket moves vertically up is equal to the weight of the bucket. As shown in figure 2.3, tension T in the hoistline if the bucket moves parallel to the static line is given by

$$T = W_B \cos \beta$$

where β, the angle of the line with respect to vertical, has a maximum value of 32.8°. However, in the middle third region of interest, β is approximately 25°. Thus, neglecting the transverse movement of the bucket overestimates T by 9 percent. The dynamic hoistline tension is independent of β as shown in figure 2.4, and is equal to the inertia force on the accelerating bucket. For the load cases considered in this investigation (sec. 2.4), the static force comprised about 72 percent of the total force in the hoistline, indicating that the error in the total force due to the assumption that the path is vertical was about 0.72 x 9, or 6 percent. Also note that this error is partially compensated by the assumption that the path of the hoistline is a straight line.

3. The hoisting cable was assumed to lie on a single straight line from the hoisting drum to the concrete bucket. This assumption has very little effect on the force in the hoistline. Figure 2.5 shows the idealization of the hoisting cable as a one-dimensional structure, under gravity loads

4

acting in directions consistent with those of the original structure. As shown in figure 2.6, the one-dimensional model gives incorrect sheave reactions, but the cable tensions are correct. Similarly, overturning moments on the cathead assembly are correct if computed using cable tensions.

4. Consistent with the initial investigation [1], the hoisting line was assumed to remain parallel with the upper portion of the static line. As shown in figure 2.7, these lines are nearly parallel.

5. The operating procedure for the hoist is such that the stresses in the hoisting cable are never compressive at any point along its length; i.e., no "snapping" of the cable is permitted. The prevention of hoist-line snapping is dictated by practical considerations to avoid derailment at the sheaves or spilling of concrete during delivery. This is corroborated by witness accounts, that no snapping of the hoisting cable was noted during the operation of the hoisting system.

6. The following quantities used in this analysis are those established during the initial investigation [1]:

a) All cable lengths and pulley locations are as shown in figure 2.1
b) the hoisting cable has an elastic modulus of 12000 ksi (82800 MN/m^2) and a cross-sectional area of 0.170 in^2 (110 mm^2)
c) The concrete bucket weighs 2900 lb (1314 kg)
d) The hoisting cable weighs 0.58 lb/ft (0.86 kg/m)
e) The maximum linear velocity of the cable at the hoist drum is 10 fps (3.0 m/s)
f) The hoist drum diameter is 16 in (406 mm).

2.3 Method of Analysis

Computation of hoisting cable forces was carried out using a computer program developed specifically for this analysis. Given the initial length of the cable, its elastic properties, and the locations and masses of the sheaves, an arbitrary time history of linear cable velocities can be applied to the hoist drum. In other words, the force applied to the drum is varied automatically as necessary to maintain the prescribed velocity history. The equations of motion are integrated step by step, using the "constant average acceleration" method. Hoisting cable tensions due to gravity are included in the analysis. If the cable is idealized as being initially taut, the weight of the bucket is included in calculating initial static tensions. If the cable is slack, the static weight of the bucket and its dynamic effects are not included initially. As the bucket is hoisted, the length of the hoisting cable decreases, changing the dynamic characteristics of the system. This change is accounted for continuously by the program. Program output includes the following as a function of time:

5

1. The velocity and acceleration of the hoist drum
2. The equivalent force required to move the hoist drum according to the prescribed velocity history
3. The dynamic tension, static tension, and total tension in the hoisting cable
   a) at the hoist drum;
   b) at the outside and inside cathead beam sheaves; and
   c) at the bucket; and
4. The displacement of the bucket above the ground, its velocity, and its acceleration.

In addition, the program also detects and outputs the maximum dynamic tension occurring anywhere in the hoistline during the lifting cycle, and the location and time at which this occurs.

After reading the input data, the program calculates the stiffness and mass matrices for the cable. Conventional truss elements are used, resulting in a tridiagonal structure stiffness matrix. Cable masses are lumped at 20 ft (6.1 m) intervals, and equivalent masses due to sheaves are added to the cable mass at appropriate locations, giving a diagonal mass matrix. Preliminary investigations showed that this discretization of mass had no effect on the accuracy of the results. The idealized structure is as shown in figure 2.8. Initially, it has 33 degrees of freedom, one for each node. As the drum takes in cable, the length of the first segment is continually updated and the stiffness and mass matrices reformed. When 20 ft (6.1 m) of cable is taken in, the first node is eliminated, and the degrees of freedom of the structure are renumbered from 1 to 32. As the bucket rises, the process continues, until as many as 10 of the original 33 nodes are eliminated.

The prescribed velocities are applied in the following manner. At the start of each time increment, the response of the system is computed assuming no load is applied to the spool end of the cable. The resulting spool velocity is V_o. Then the response of the system is recomputed assuming a unit force F_1 applied to the hoist end, giving a hoist velocity V_1. If the prescribed velocity from the assumed velocity profile is V, the hoist force necessary to produce it is given by

$$ F = \frac{V - V_o}{V_1 - V_o} \cdot F_1 $$

This force is applied to the hoist end of the cable, and the response is computed. Dynamic cable tensions are computed using the stiffness of each segment. Cable tensions due to gravity loads are calculated, taking into consideration the displacements of the bucket. Total cable tensions are obtained by summing up the corresponding dynamic and static values. The process continues until the bucket reaches a height of 200 ft (61 m).

2.4 Load Cases Investigated

Load Case A: Initially Taut Cable (Refer to fig. 2.9) - Lower Bound
            Condition

The hoist drum and cable have zero initial velocity and they initially
carry tension due to the static weight of the concrete bucket plus the
cable self weight. Starting from these conditions, the equivalent linear
velocity of the drum is increased to 10 fps (3.0 m/s) sinusoidally over
a time interval varying from 2 to 8 seconds. Two seconds represented
the shortest time interval which did not produce snapping of the hoist-
ing cable. Preliminary runs showed that for a given load case, integration
time steps less than or equal to 0.025 sec gave very similar results
as long as the cable was considered initially taut. A time step of 0.025
sec was therefore used for this type of load case.

Load Case B: Initially Slack Cable (Refer to fig. 2.10) - Upper Bound
            Condition

The hoist drum and cable have a prescribed initial velocity but do not
carry any initial tension. Starting from the prescribed initial velo-
city, the mass of the concrete bucket is immediately applied to the
hoisting system, the weight of the bucket is included in computing
static tension, and the hoisting drum velocity is increased to 10 fps
(3.0 m/s) over a time interval from 2 to 8 seconds. Preliminary runs
showed that for a given load case, integration time steps less than or
equal to 0.005 sec were required to obtain satisfactory convergence of
results, and that time step value was therefore used for this type of
load case. Based upon the assumption that the cable did not snap during
hoisting, the total force in the hoisting cable at any point along its
length was never allowed to become compressive. When the cable was
considered initially slack, initial velocities exceeding 4 fps (1.2 m/s)
were found to cause subsequent snapping of the cable. During the quickest
lift, in which the prescribed velocity was increased from 4 fps (1.2
m/s) to 10 fps (3.0 m/s) in a 2-sec time interval, the total hoistline
force became slightly compressive several times for very short lengths
of time (less than 0.02 sec). These momentary compressive forces were
about 100 lbf (445 N) in magnitude.

2.5 Discussion of Results

Table 2.1 shows the maximum values for the following forces occurring
during the hoisting of the concrete bucket:

7

1. Tension in the hoisting cable.
2. Unbalanced load applied to the cathead due to different hoisting cable forces at each cathead sheave. This is shown as (T_1-T_2) in figure 2.12.

As can be seen from table 2.1, the most severe loading in the hoisting cable occurs for the case in which the cable is initially slack, the maximum dynamic tension being 4.1 kips (18.2 kN). It should be noted that this maximum occurs when the concrete bucket has displaced 150 ft (46 m) from the ground. Prior to this, the hoisting cable experiences repeated dynamic tensions of about 3.5 kips (15.6 kN).

If the cathead assembly does not deflect, changes in hoisting cable tension produce no change in the static line tension, as the hoistline will always remain parallel to the upper portion of the static line (fig. 2.7). However, dynamic variations in tension along the length of the hoistline do produce overturning moments on the cathead, which lead in turn to deflections of point G, at the top of the static line. These deflections do influence static line forces.

According to the initial study (see table 6.1, ref. 1) the static line tension decreases by about 12 percent (from 5.4 kips, 23.9 kN to 4.8 kips, 21.2 kN) when the elastic deformation of the cathead is considered. Table 2.1 shows that the maximum difference in the hoistline tensions at the cathead sheaves is 1.6 kips (7.1 kN). However, as in the case of the maximum hoistline tension, this maximum occurs only once (initially) and the repeated maximum difference in tension at the cathead is about 1.0 kip (4.5 kN) in either direction, when the bucket is in the middle third region where the total load effects are greatest. Considering the governing direction (same as static line tension), the 1.0-kip (4.5-kN) force difference produces an additional moment on the shell but decreases the static line tension by about 2.5 percent (12% of 1.0 kip $\simeq$ 2.5% of 4.8 kips). While all of these forces would be decreased somewhat if damping were included in the model, they are far more sensitive to the assumed hoisting procedures.

3. CONCRETE STRENGTH REQUIREMENTS IN DESIGN

3.1 Design Philosophy

The basic requirement in the design of any structure is that it should safely support all loads during construction and in service. The imposition of construction loads on a partially completed structure should, therefore, be subject to the same basic consideration given to the

8

design of completed structures under service loads. For the particular case of cooling tower construction, the designer of the construction system should first evaluate the peak construction loads, including dynamic effects, that will be imposed upon the partially completed concrete tower; and secondly, determine the required strength of the concrete to support the imposed loads with a margin of safety comparable to that incorporated in the design of concrete structures in general.

3.2 Evaluation of Construction Loads

In the initial study [1], five basic load types were considered acting on the tower. These were: (1) the self-weight of the tower, (2) the dead load of the suspended scaffold and formwork system, (3) live loads on the scaffold, (4) weight of cathead assemblies and (5) hoisting loads. In this study, only the hoisting loads need to be reevaluated to account for dynamic effects considered in the preceeding section.

As shown in the table 2.1 and explained in section 2.4, the lower and upper bound values of the maximum dynamic forces in the hoisting cable (load cases A and B, respectively) are associated with two different hoisting procedures. From a practical standpoint, it is reasonable to assume that the bucket is brought up to speed (to 10 fps or 3 m/s) in the least amount of time without causing snapping of the hoistline. This represents an operating procedure which minimizes delivery time while keeping the movement of the bucket under control to avoid mishaps such as splashing of concrete or derailment at the sheaves. In both load cases A and B, this minimum time interval is two seconds (figs. 2.9 and 2.10). It should be pointed out that dynamic load effects on the hoistline system increase as the time interval used to accelerate the bucket decreases.

The first two columns of table 2.1 list the respective values of maximum dynamic and total (static and dynamic) tensions in the hoistline. In every load case this maximum tension occurs at the drum while at other locations, including the bucket end, the maximum tension is less. Because the dynamic component of the tension at the bucket end is assumed parallel to the segment of the static line above the bucket, it will have no effect on the static line tension, as pointed out in section 2.5.

Among the load cases considered, the maximum tension in the hoistline is 7.0 kips (31.2 kN) and occurs under load case B. The breaking strength of the hoistline cable (27 kips or 120 kN, see sec. 5.2, ref. 1) is several times of this value and therefore, sufficient to resist the peak dynamic effects considered.

At any given time during hoisting operations, the parameters $T_2 - T_1$ and $T_2 + T_1$ (fig. 2.12) provide an indication of dynamic load effects on the shell. It is recalled that in the static analysis of hoisting loads, tension F_D in the hoistline was treated as constant and therefore, contributed mostly to axial (meridional) forces F_y but not to normal forces F_x which produce overturning moments on the shell (see sec. 6.7,

9

ref. 1). In dynamic analysis, the maximum value of $T_2 - T_1$ is of significance because it produces additional overturning moments not accounted for in the static analysis. On the other hand, the difference $(T_2 + T_1)_{max} - F_D$, if positive, will produce additional axial forces which, likewise, were not accounted for in the static analysis.

The last column of table 2.1 lists the maximum values of $T_2 - T_1$ for the various dynamic load cases. For load case A, this difference and its effect on the shell is negligible. For load case B, the maximum difference is 1.6 kips or 7.1 kN (table 2.1). However, it was noted earlier that the static line tension due to static load is at or near its peak value when the bucket is within the middle third region of the static line. The results of dynamic analysis for load case B show that during the time interval when the bucket is located within this middle third region the maximum difference $T_2 - T_1$ is 0.8 kip (3.6 kN) while the corresponding sum $T_2 + T_1$ is 3.0 kips (13.4 kN). However, the governing loading condition occurs when $T_2 + T_1$ is maximum and is equal to 7.4 kips (32.9 kN). The corresponding difference $T_2 - T_1$ is 0.6 kip (2.7 kN). These were the values used in subsequent calculations of dynamic load effects on the shell.

With a minor modification, the special purpose program developed for the static analysis of hoisting loads (sec. 6.7, ref. 1) was also used to compute the dynamic load effects on the shell. The program was altered to analyze hoisting loads using different values for T_2 and T_1 specified by input. This analysis yielded the results shown in table 3.1. The last stage in the conversion of hoisting loads (load case 5) into equivalent actions applied directly to the shell, according to the procedure described in section 6.2 of ref. 1 leads to the results shown in table 3.2.

3.3 Evaluation of Required Concrete Strength

It was shown previously [1] that maximum stresses occurred in the region of the panel bounded by the two ribs where cathead no. 4 was located. That analysis showed that combined stresses resulting from the hoop forces and bending moments near the top of the shell and meridional forces and bending moments near the bottom of lift 28 exceeded the capacity of the shell. It was concluded from that analysis that failure of lift 28 was initiated because the strength of concrete was not adequate to develop the necessary capacity to resist the applied construction loads. The inadequate capacity of the shell at the above mentioned critical locations was shown by means of interaction diagrams of axial force and bending moment. The combinations of stress resultants at the critical locations exceeded the ultimate capacity of the cross section. Interaction diagrams are also used herein to determine the ultimate strength of concrete necessary to develop adequate capacity of the shell to resist safely imposed construction loads.

The failure envelope for a given reinforced concrete section may be represented qualitatively by an axial force (N)-bending moment (M) interaction diagram of the type shown by the solid curve in figure 3.1 (for further explaination consult sec. 7.2 and fig. 7.1 of Ref [1]). The design envelope, shown dotted in the figure, defines the limiting conditions required to maintain a factor of safety of 2.0 against failure. Graphically, this means that the design curve will bisect any radial line from the origin to the failure envelope. A particular radial line simply represents the locus of all points for which the ratio N/M is constant and is equal to the slope of that line. The slope of line 0-1-2 shown, for instance, is given by the ratio N_1/M_1 or N_2/M_2. Note that in this case (N_1, M_1) and (N_2, M_2) represent load combinations at the design and ultimate levels, respectively (points 1 and 2 in the figure), so that the ratios N_2/N_1 and M_2/M_1 have the same value as the specified factor of safety.

The design strength of the shell should be such that the capacity of any section of the partially completed tower exceeds the construction load effects by a reasonable margin of safety. In this analysis a factor of safety of 2.0 is used, and is derived by the combination of an appropriate load factor and strength reduction factor ϕ. For members subjected to axial compression with flexure, the ACI 318-77 Code [2] recommends ϕ values which vary between 0.7 and 0.9, depending on such factors as the type of load effects and the amount, symmetry and layout of the reinforcement. These values are applicable to concrete structures in service. Considering the greater variability of strength that partially cured concrete exhibits relative to that based on 28-day strength tests, a strength reduction factor of $\phi = 0.7$ for young concrete of the Willow Island tower is judged to be appropriate. The ACI Code also recommends load factors in the design of concrete structures under service conditions. Although a final decision from the code authorities on an acceptable construction load factor has not been made, there is evidence of increasing consensus toward adopting a construction load factor somewhere in the range of 1.3 to 1.4. The higher value of 1.4 is adopted in this investigation recognizing the possible variability of dynamic effects on hoisting loads indicated in table 2.1. The division of this load factor by the strength reduction factor of 0.7 yields the safety factor of 2.0 used in this study.

To determine the strength of concrete which is necessary to develop adequate resistance to the applied construction loads without failure, an iterative procedure was followed using the shell analysis program described in section 6.9 of reference 1. This procedure was necessary because the stress distribution in the shell varies with changes in the stiffness of the shell. In other words, as the concrete strength increases, the elastic modulus also increases, which in turn changes the stress distribution in the shell. Because the rate of increase in the elastic modulus in each of the lifts of the tower varies according to the age of curing, a number of independent analyses are necessary to reflect redistribution of stresses in the shell with different values of stiffness for each lift. Changes in axial forces and bending moments

11

due to changes in the compressive strength of concrete, hence the stiff-ness, at a number of critical locations (A, B, C and D shown in fig. 4.2) are listed in table 3.3 for a selected number of concrete strengths. Note that meridional axial forces and bending moments at points A and B decrease as the strength of concrete increases, while the corresponding hoop values at points C and D increase. A comparison of the values of the first two rows shows the change in axial forces and bending moments as a result of the inclusion of the dynamic force (sec. 2.4) due to hoisting. As seen in the table, no significant changes in axial forces and bending moments occur.

The values listed in the first two rows of table 3.3, which are based on the 220-psi (1.52 MPa) predicted concrete strength in lift 28 at the time of failure, are plotted on the interaction diagrams corresponding to concrete strengths of 1000 psi (6.9 MPa) and 4000 psi (27.6 MPa) in figures 3.2 and 3.3. In these figures the ultimate bending moment of the shell cross section is mainly controlled by the amount of reinforce-ment and its location. Consequently, a substantial increase in the concrete strength would not correspondingly increase the bending capacity of the shell cross section.

In figure 3.2 points A and A' correspond to a combination of meridional axial force and bending moment for location A obtained without and with the dynamic force effect included in the analysis, respectively (first two rows of table 3.3). A" corresponds to the case in which a factor of safety of 2.0 is applied to the axial force and bending moment for point A'. As in the cases of A, A' and A", the same explanation also applies to points B, B' and B". B''', however, corresponds to the point which represents a combined axial force and bending moment capacity with a factor of safety of 2.0 corresponding to a compressive strength of 4000 psi (27.6 MPa) and a modulus of elasticity corresponding to that strength. Note that the difference between points B''' and B'' is due to the different elastic moduli used in their calculations.

It is clearly seen from the figure that the strength of the horizontal cross section, i.e., the cross section perpendicular to the meridional axis, is predominantly governed by bending moment. At a compressive strength of 1000 psi (6.9 MPa), the lower portion of the panel (point B in fig. 4.2) where cathead no. 4 was located would begin to experience crushing of concrete. For a margin of safety of 2.0 against development of crushing with the inclusion of the dynamic force effects, the concrete should develop 4000-psi (27.6 MPa) strength.

In figure 3.3, points C and D correspond to a combined condition of hoop axial force and bending moment at locations C and D of the panel, C' and D' correspond to the case where the dynamic force is included in the computation of axial force and bending moment, and C" and D" represent the case where a factor of safety of 2.0 is applied to the axial force and bending moment for points C' and D'. It is seen in the figure that the vertical cross section at locations C and D would not experience crushing at a compressive strength of concrete of 1000 psi (6.9 MPa),

and the minimum concrete strength of 4000 psi (27.6 MPa) that would be required to maintain a factor of safety of 2.0 against crushing failure at point B is well beyond the strength required to maintain a factor of safety of 2.0 aginst crushing at location D in the shell (point D" in fig. 3.3).

Based on the foregoing analysis it is concluded that crushing failure would occur if the concrete strength in lift 28 is 1000 psi (6.9 MPa) or less, and that in order to resist the applied loads with a factor of safety of 2.0 against crushing failure of the shell the concrete strength in lift 28 should be 4000 psi (27.6 MPa). It should be recognized that these concrete strengths are not demarcation lines which divide "safe or unsafe" condition. As the strength of concrete decreases from 4000 psi, the factor of safety will likewise decrease. The factor of safety will approach to 1.0 as the concrete strength decreases toward the 1000 psi level, and at that level conditions would be such that failure is immenent.

4. EFFECT OF ADDITIONAL BOLTS ON TOWER RESPONSE

In the initial investigation of the Willow Island cooling tower collapse, it was established that the lowest line of bolts between the exterior jumpform beams and the shell were not in place at the time of failure. The location of these bolts is indicated in figure 4.1 which shows a typical profile of the scaffolding and cathead assembly at the top of the tower. The purpose of the following investigation is to assess the effect of these bolts on the response of the tower to the applied construction loads. This was not part of the scope of the original report because the structure was considered as it was without any changes that might have altered its response.

An additional line of bolts will cause a redistribution of part of the applied loads to points below the top anchor line in lift 27 (fig. 4.1) and thereby alter the stress resultants at the critical sections in the shell, represented by points A through D in figure 4.2. Assuming the bolts are in place, and noting that the applied construction loads tend to pull the tower down and toward the inside, any shear or tensile stresses transmitted to these bolts would indicate possible relief in the meridional stress resultants (N_ϕ, M_ϕ) at critical points A and B as well as in the hoop stress resultants (N_θ, M_θ) at critical points C and D (fig. 4.2).

As noted in section 6.3 of ref. 1, the axial stiffness of the shell is several times that of the jumpform beams. Therefore, a compressive force applied to the cantilever portion of the exterior jumpform beam (fig. 4.1) will be taken up mostly by the top anchor bolt in lift 28 acting in shear. Similarly, a compressive force applied between the top and bottom bolts in lift 28 will be shared mostly by these two bolts. In either case, the difference will be taken up mostly by the next lower bolt and so on, so that any shear force transmitted to the lowest bolt in lift 27 will be negligible. Thus, it is concluded that the addition of a fourth bolt does not alter significantly the shear forces in the meridional direction in the remaining bolts.

The inside flange of the exterior jumpform beam, which incorporates a U-shaped rib mold (fig. 4.3), fits tightly against the concrete rib and thus inhibits torsional deformations of the beam as well as flexural

deformations about its minor axis. As a result, any loads producing
these effects will remain localized. It is therefore concluded that
the presence of a fourth bolt does not alter significantly the distri-
bution of applied torques and axial forces to the portion of the shell
above lift 27.

Flexure of both the exterior and interior jumpform beams about their
respective major axes and the associated shears are the only other
effects which remain to be considered. Therefore, the pair of jumpform
beams, together with the interconnecting anchor bolt assemblies (fig.
4.1) can now be modelled as a two-dimensional (plane) frame as shown in
figure 4.4.

In the model, all joints are assumed continuous except the hinge at node
7 which connects the top and bottom sections of the exterior jumpform
beam. The assumption of continuity does not introduce appreciable
errors in the analysis because the flexural rigidity of the anchor bolts
is very low relative to the beams. Points I, J, M and N designate the
locations of the four anchor bolts through the shell, from top to bottom,
respectively. K and L are intermediate load points in lift 28. The dis-
tance between the exterior and interior jumpform beams (top and bottom
beams in the model) with respect to the centerline of the shell is
assumed to be the distance to the respective centroids of the jumpform
beams. The actual length of the anchor bolts are therefore shorter than
those in the model. To compensate for the difference, the axial rigidity
of the actual anchor bolts is used in the analysis. The loads shown are
the same as before (sum of load cases 2 through 5, sec. 6.1, ref. 1).

The condition of compatibility imposed upon the model is that beam dis-
placements should conform with the normal displacements of the shell.
The deflected shape of the shell relative to its normal displacement
at anchor point N is shown in figure 4.4. This curve is developed on
the basis of normal displacements of the shell obtained in the initial
study. In addition, the beams are not allowed to displace into the space
occupied by the shell between nodes 8 and 37. That is, the beam nodes
8 and greater are allowed to deflect away from the "sandwiched" shell
but not into it. This requires an iterative procedure whereby initially
some of the nodes 8 to 37 are assumed to be in contact with the shell
while the others are assumed to move away from its surface so that they
are free to rotate and translate. The frame is then analyzed with the
aid of the computer and a general purpose structural analysis program
by imposing the known shell displacements at all the nodes that were
assumed to be in contact with it. The results of successive analyses
are then modified by imposing or removing the appropriate nodal displace-
ments in a manner that maintains the above-cited compatibility require-
ments, until the results obtained from a particular run turn out to be
consistent with the displacement assumptions made for that run.

The results of the final analysis indicate that the additional bolt,
assumed present at N, will develop a tensile force of 1998 lbf (8819 N).
The actions (forces and moments) on the portion of the frame to the right

14

of the anchor bolt at J are shown in figure 4.4. It is recalled that these actions were not present in the initial investigations because the bolt at N was not in place. The corresponding reactions at anchor bolt locations I and J are indicated in the same figure. These reactions are calculated by assuming I and J are simple supports, similar to the procedure used in the initial investigation (see sec. 6.3 of ref. 1).

Table 4.1 compiles the sum of external actions on the shell. These were obtained by combining the actions corresponding to load cases 2 through 5 tabulated in figure 6.6 of reference 1. In table 4.1, the figures shown in parentheses are the revised forces at I and J in the x direction (normal to the shell) as a result of the addition of a bolt at N. They are obtained by combining algebraicaly the reactions at I and J shown in figure 4.4 with the tabulated forces F_x (those without parentheses) from the initial study. None of the other actions is altered for reasons discussed earlier in this section.

Note that the addition of a bolt at the base of lift 27 (location N, fig. 4.4) reduces the magnitudes of the forces at I and J in the normal direction by about 10 and 22 percent, respectively, while leaving the other actions unaltered. An analysis of the shell using the new set of loads in table 4.1 as input together with the SHORE III program (see app. B, ref. 1) yields the stress resultants at critical locations A through D in lift 28 (see fig. 4.2). The meridional stress resultants (M_ϕ, N_ϕ) at A and B are shown on the interaction diagram of the concrete section at these points in figure 4.5. The corresponding results of the initial study (without the lower bolt) are shown in the same figure for comparison. In a similar manner, the hoop stress resultants (M_θ, N_θ) at C and D are plotted in figure 4.6 along with the corresponding results from the initial study.

A comparison between the two sets of results indicates that failure in lift 28 at catheat no. 4 will have occurred under the same set of construction and loading conditions even if an additional bolt was used between each exterior jumpform beam and lift 27. Although the magnitudes of the critical stress resultants at B and D are reduced to some extent by the additional bolt, they are still well beyond the ultimate capacity of the concrete section in lift 28 at both these locations.

5. EFFECT OF STATIC LINE RELOCATION ON TOWER RESPONSE

The ground anchor point of the static line was moved to a point near the center of the tower base on April 17, 1978. Lift 26 was the first section of the tower placed on April 19, 1978, after the ground anchor point had been moved. Lift 27 was placed on April 24, 1978, 5 days after the placement of lift 26, and lift 28 was placed on April 26, 1978, 2 days after the placement of lift 27. Failure in lift 28 occurred when lift 29 was being placed on April 27, 1978. Lift 28 was the first section of the tower which was cured for less than one day prior to formwork removal after the ground anchor point had been moved to the center of the tower base.

15

The analysis of the effect of moving the ground anchor point of the static line at its previous location on the magnitudes of the critical stresses in the shell closely parallels the procedure in the first study and consists of four basic steps: (1) definition of geometry and stress-free length of the static line; (2) evaluation of maximum hoisting loads using the special purpose cable analysis program developed in the first study; (3) evaluation of the stress resultants in the shell using the SHORE III shell analysis program; and (4) comparison of the stress resultants with the previously established sectional capacity of the concrete shell.

Figure 5.1 shows the geometric layout of the static line. Point B_1 represents the position of its ground anchor point before the last move to position B following the casting of lift 25. The space coordinates of point B_1 were calculated on the basis of field survey data supplied by OSHA. To assist in the visualization of the hoisting and scaffolding system setups, figures 6.3 and 6.1 in reference 1 have been reproduced as figures 2.1 and 2.7 in this report with slight modifications to reflect the shift in position from B to B_1.

The criterion for deriving the stress-free length of the static line can be visualized by reference to figure 2.7. With the concrete bucket at the unloading position shown, and the static line assumed tensionless but without play for that position, the stress-free length is represented by the line GKB_1, as shown. This length can be calculated from the known coordinates of points G and B_1 (fig. 5.1) and the position of point K which is also known. The stress-free length of the static line calculated according to this procedure is 196.36 ft (59.89 m).

It should be noted that the stress-free length of the static line used in the initial investigation was obtained by direct measurements in the field. However, the calculated length according to the above criterion turned out to be almost identical to the measured length, the difference being 0.02 ft (6 mm). There are practical considerations that limit the tolerance in the amount of play in the static line as discussed in section 6.7 of reference 1. Therefore, the calculated stress-free length of 196.36 ft (59.89 m) is sufficiently accurate for the purpose of this analysis.

Because the procedure from this point on is identical to that described in reference 1, only the results will be discussed. Figure 4.2 shows the locations in lift 28 where the calculated stress resultants are maximum. At points A and B, the meridional stress resultants (N_ϕ, M_ϕ) govern.

Figure 5.2 shows the interaction diagram for the concrete strength f_c' = 220 psi (1.52 MPa) defining the failure envelope for horizontal concrete sections of unit width at points A and B. The maximum calculated stress resultants (N_ϕ, M_ϕ) at these points are plotted in the same figure as indicated. As both these points fall well within the failure envelope, it is concluded that, with the static line anchor at B_1, the construction loads will not produce failure in lift 28 along the horizontal plane

16

through points A and B which represent locations where the most critical meridional stress resultants occur in the shell.

Figure 5.3 shows the failure envelope for vertical concrete sections of unit width at the level of points C and D for f_c = 220 psi (1.52 MPa). The maximum hoop stress resultants (N_θ, M_θ) induced at these points are plotted in the same figure as shown. It is noted that both these points lie within the region defined by the solid line interaction diagram which has been developed based on the assumption that no splicing of horizontal bars occurs within the region of interest (points C and D in this case). If it is assumed that splicing of horizontal bars occurs in the critical region of interest, the sectional capacity will be represented by the dotted interaction diagram shown in the same figure. It is seen that even if splicing occurs, the induced stress resultants at points C and D would still fall within the capacity of the concrete section. However, in view of the proximity of point D to the failure envelope, a slight overstress could cause local crushing of the concrete section in the vertical plane in that region.

The possibility of excessive radial shear stress resultants on horizontal and vertical sections at the critical points were also investigated. The induced shear stresses were found to be approximately within 50 percent of the available sectional shear capacity. The procedure followed was that described in section 7.3 of reference 1. The possibility of shear failure was therefore ruled out.

In the light of the foregoing discussions, the following conclusions may be drawn. If the base anchor point of the static line had been kept at its previous location (before the last move to near the center of the tower), the effects of the construction loads would have been reduced to such an extent that failure of lift 28 of the tower would probably not have occurred.

It must be recognized that in the above analysis, possible dynamic effects on the hoisting loads were not considered because of insufficient factual information. However, as indicated by the analysis discussed in section 3, such dynamic effects will only slightly amplify the stress resultants in the shell. Consequently, the conclusions cited above will not be altered by consideration of dynamic load effects.

6. SUMMARY AND CONCLUSIONS

The analysis presented in this report responds to questions on various construction aspects of the Willow Island cooling tower that were not part of the scope of the original investigation [1]. That investigation considered conditions as they existed at the time of the collapse in order to determine its most probable cause while this analysis goes beyond that investigation by considering changes to those conditions and their effect upon the response of the tower. It should be emphasized that all of these investigations and conclusions drawn are valid only

for the specific case of the tower analyzed. The questions in this investigation address the following specific topics:

1. The strength of concrete that would be required in lift 28 of the tower in order to resist the applied loads with a reasonable factor of safety and with due consideration given to the dynamic nature of the loads.

2. Possible effects of an additional line of bolts between exterior jumpform beams and the shell at the base of lift 27.

3. Possible effects of a shift of the anchorage point of the static line back to the location just prior the last move to the center of the tower.

To answer the first question, hoisting loads were modified to include dynamic effects which were evaluated by a separate analysis. Next, the stress resultants in the shell due to the revised loads were determined by analysis and were compared with the resistance of the shell for each increment in the compressive strength of the concrete throughout the shell profile. Because the stiffness of the shell increases with compressive strength, an iterative procedure was followed that took into account changes in both strength and stiffness. The results of this analysis showed that crushing failure would initiate in lift 28 if the concrete strength in that lift is 1000 psi (6.9 MPa) or less. On the other hand to maintain a factor of safety of 2.0 against crushing failure, the concrete in lift 28 should have been allowed to develop a comprehensive strength of 4000 psi (27.56 MPa).

To answer the second question, the problem was analyzed with the lowest bolt in place by using a two-dimensional rigid frame model to represent one of the two pairs of jumpform beams, as well as the four interconnecting anchor bolts through the shell. The model was subjected to the construction loads and constraints corresponding to the normal deflections of the shell determined in the initial study [1], as well as to constraints that did not allow the displacement of any part of the jumpform beams into the shell. The results of this analysis indicated that due to the presence of the additional bolts in lift 27 the magnitudes of the critical stress resultants were reduced to some extent, but were still well beyond the ultimate capacity of the concrete section in lift 28. It is therefore concluded that even under these conditions, the concrete in lift 28 would have failed.

To answer the third question, an analysis was performed following the steps of the initial investigation, with the ground anchor point of the static line moved back to the location prior to its last move. The results of this analysis indicated that if the base of the static line were kept at its previous location, the critical stress resultants would have been significantly less than the ultimate strength of the concrete section in lift 28. It is therefore concluded that the concrete in

18

lift 28 would probably not have failed and consequently, collapse would not have occurred.

7. ACKNOWLEDGEMENTS

8. REFERENCES

1. Lew, H. S., Fattal, S. G., Shaver, J. R., Reinhold, T. A., and Hunt, B. J., "Investigation of Construction Failure of Reinforced Concrete Cooling Tower at Willow Island, W. Va.," NBSIR 78-1578, National Bureau of Standards, Washington, D.C. 20234, November 1979.

2. ACI 318-77, "Building Code Requirements for Reinforced Concrete," American Concrete Institute, Detroit, Michigan, 1977.

Table 2.1 Summary of maximum forces in the hoistline (kips)

Loading Description	Load Case	Hoisting Cable		Cathead
		Maximum Dynamic Tension	Maximum Total Tension*	Maximum Unbalanced Load
Initially taut cable initial velocity = 0 fps accelerated to 10 fps in 2 sec.	A	1.1	4.0	0.02
Initially slack cable initial velocity = 4 fps time interval to 10 fps = 2 sec.	B	4.1	7.0	± 1.6

(1 kip = 4.45 kN)

* Maximum total tensions occur at the hoisting drum.

Table 3.1   Cathead forces and reactions due to
dynamically amplified hoisting loads
(revised load case 5)

Impact Factor	3.4/2.9 = 1.17
Support Condition at G	Elastic
W_B – weight of bucket	3400 (1540)
S_o – stress-free length of static line	219.17 (66.80)
F_D – tension in hoistline	2942 (13092)
T – tension in static line	4766 (21209)
F_c – tension in counterstatic line	10511 (46774)
A_p – ⎱ cathead leg	17681 (78680)
B_p – ⎱ reaction	931 (4143)
A_z – ⎰ components	3277 (14583)
B_z – ⎰ (fig. 6.12, ref. 1)	181 (805)
L_1 – static line chord lengths below	90.00 (27.45)
L_2 – and above bucket (fig. 6.10, ref.1)	128.56 (39.21)

Units   Force: lbf (N)
           Weight: lb (kg)
           Length: ft (m)

Table 3.2   Load case 5 – revised hoisting loads

Location Forces	I	J	K	L
F_x (lbf)	-19819	12766	422	3075
F_y (lbf)	-2199	-2199	0	0
F_z (lbf)	2302	-2302	758	-1602
M_y (ft-lbf)	829	829	1291	2194

(1.00 lbf = 4.45 N, 1 ft-lbf = 1.36 N•M)
* Actions and location of points defined in
  Figure 6.6, Ref. [1].

Table 3.3 Change in axial forces and bending moments due to
increasing compressive strength of concrete*

Comprssive Strength psi	A		B		C		D	
	N_ϕ kip	M_ϕ kip-in	N_ϕ kip	M_ϕ kip-in	N_θ kip	M_θ kip-in	N_θ kip	M_θ kip-in
220 **	-0.02	54.31	3.81	89.52	27.11	2.45	31.91	76.42
220	-0.06	56.39	3.88	92.87	28.10	2.68	32.99	79.58
500	-0.03	53.68	3.83	90.82	29.50	6.10	34.41	82.13
1000	0.00	50.75	3.77	88.52	30.94	10.11	35.88	85.06
2500	0.05	47.53	3.73	85.88	32.33	15.47	37.32	89.27
4000	0.07	46.66	3.72	85.13	32.60	17.48	37.61	91.07

* Tabulated values of axial forces and moments occur on a 1-ft long section
of shell: (1.0 kip/ft = 14.6 kN/m ; 1.0 kip-in/ft = 0.37 kN-m/m).

** With the exception of the first row of data, tabulated values include
the effects of the dynamic forces in the hoisting cable.

Table 4.1 Sum of external loads on the shell

Location Forces	I	J	K	L
F_x	-20655 (-18501)	13234 (10250)	494	2970
F_y	-6320	-6320	0	0
F_z*	2364	-2274	778	-1610
M_y*	865	864	1344	2206

* Near side jumpform beam
   (force at far side equal and opposite)

Units: Moment in ft-lbf (1.00 ft-lbf = 1.36 N·M)
        Force in lbf (1.00 lbf = 4.45 N)

Numbers in parentheses are revised forces
assuming lower line of bolts is in place
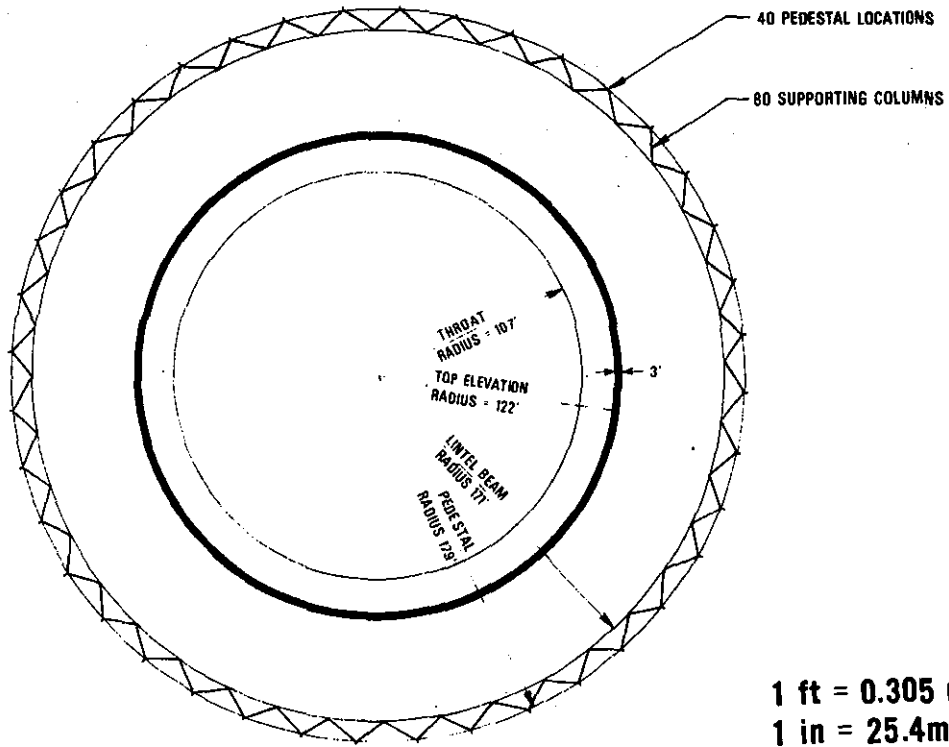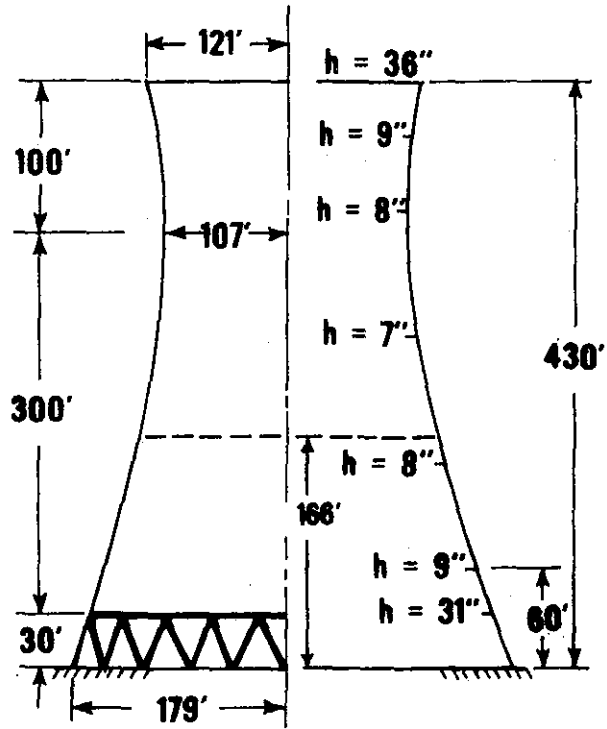
Figure 1.1   Elevation and plan view of the cooling tower

1 ft = 0.305 m
1 in = 25.4mm

24
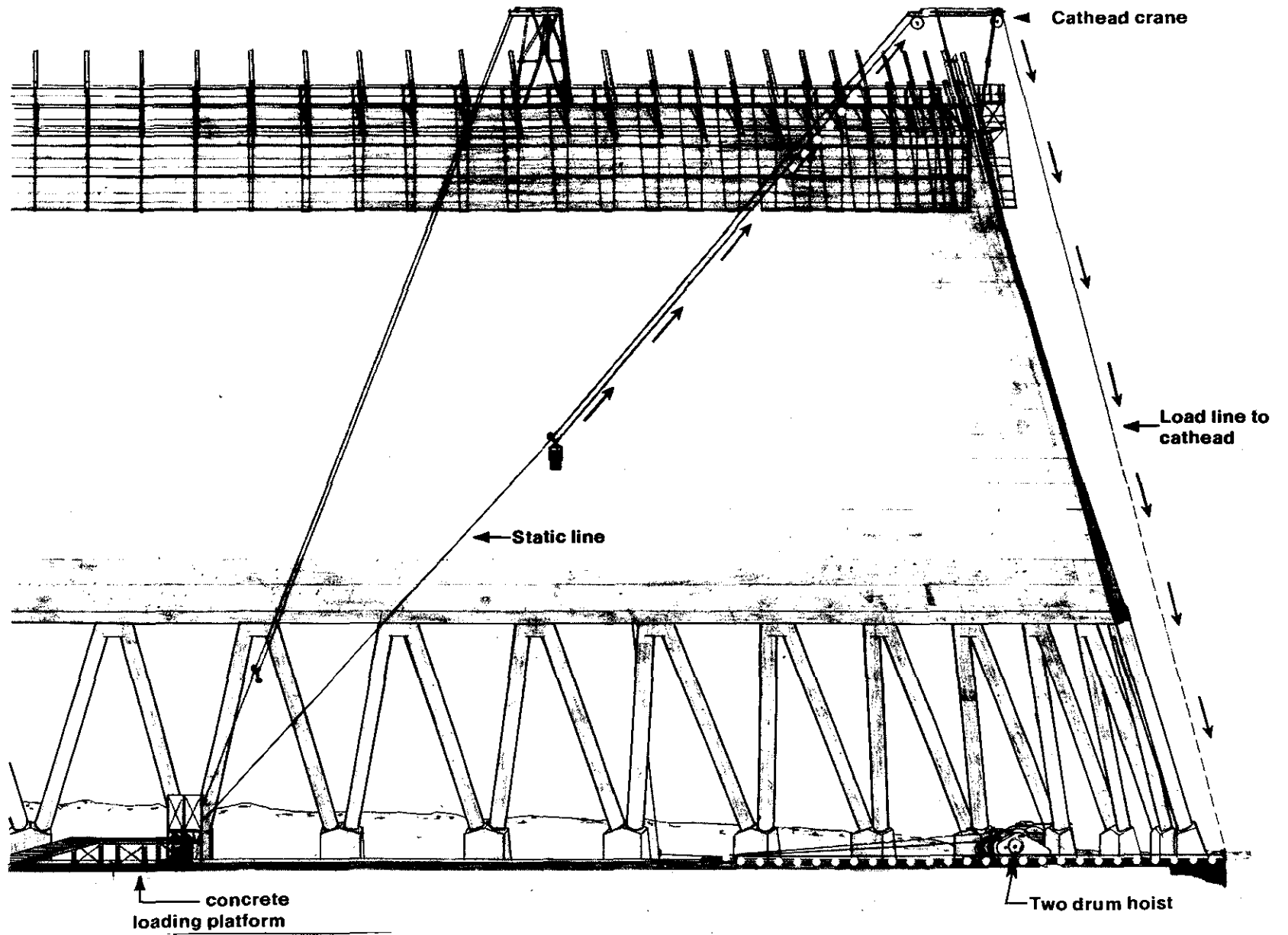
Figure 1.2   Schematic view of construction and hoistion system layout

FIELD DATA

Figure 2.1 Layout of hoisting system
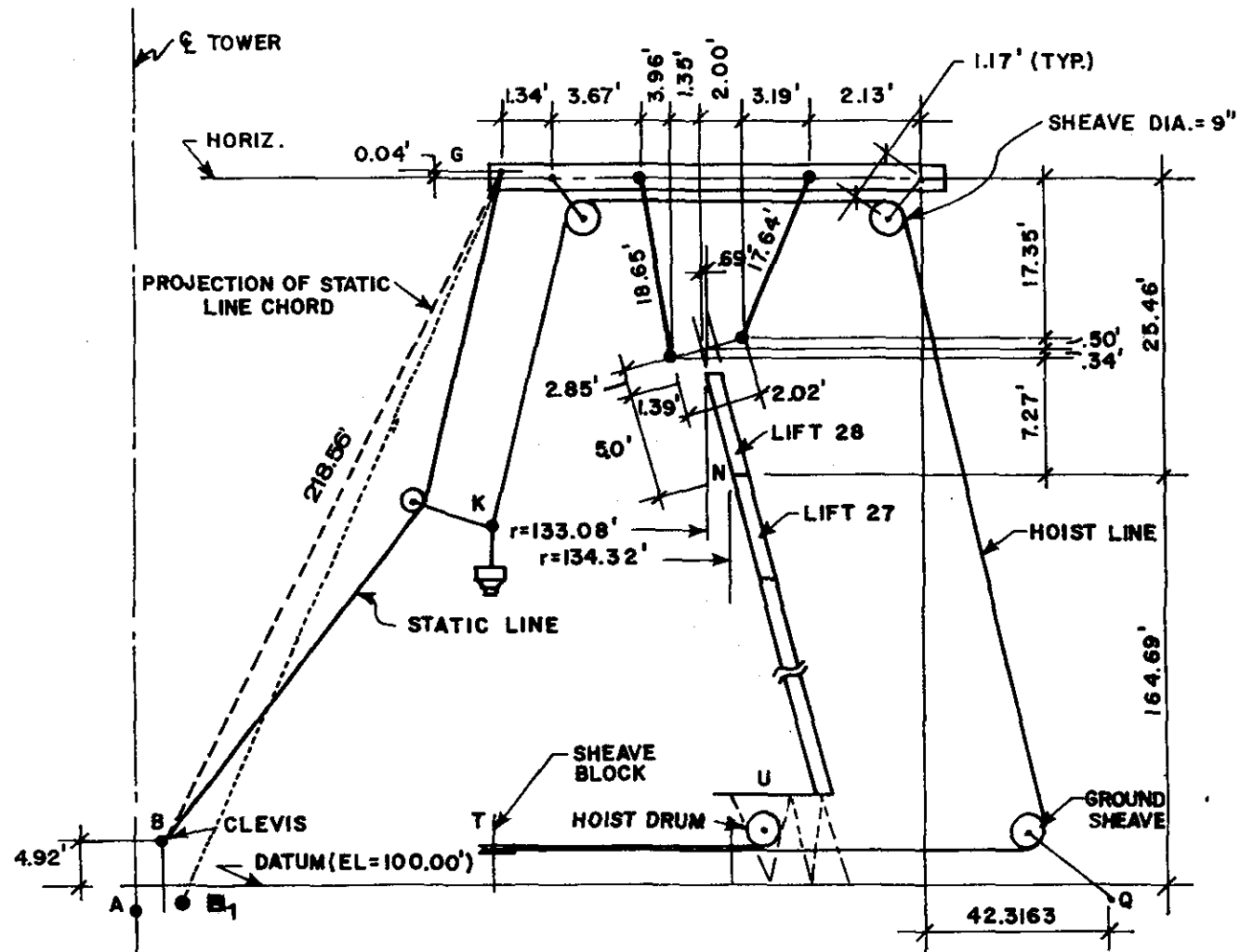
1.0 ft = 0.305 m

LENGTH OF HOIST LINE (UK) AT CATHEAD 4 = 470.4 FT.
LENGTH OF HOIST LINE AT CATHEAD 5 = 408.6 FT.

$$\beta = \tan^{-1}(120/186) = 32.8° = 0.573 \text{ rad}$$

1 ft = 0.305 m
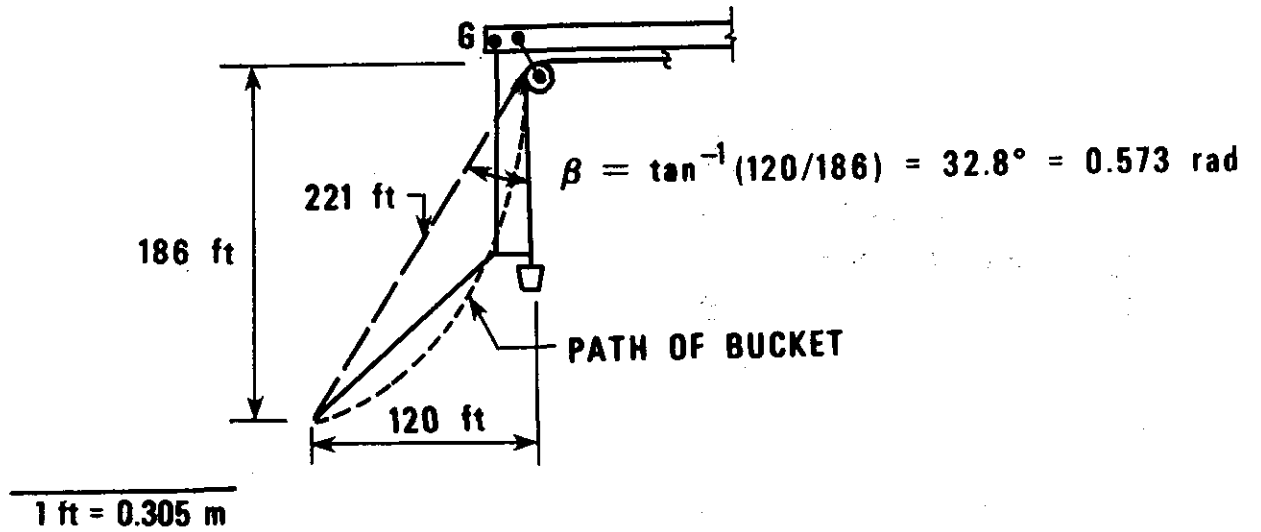
Figure 2.2   Path of the bucket

$$T = W_B \cos \beta$$
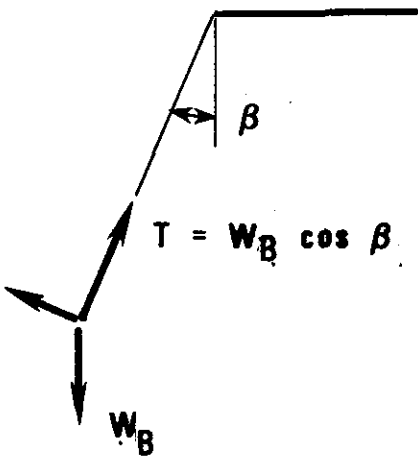
Figure 2.3   Hoistline tension due
to static loads

FDYN

INERTIA FORCE ON
ACCELERATING BUCKET
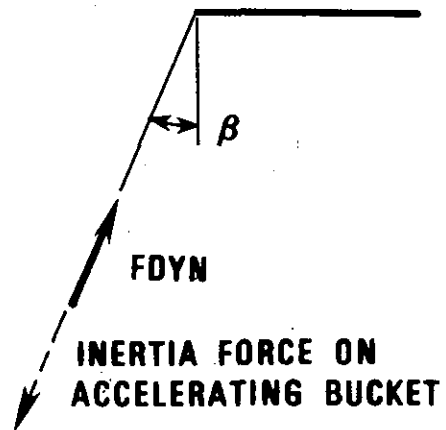
Figure 2.4   Hoistline tension due
to dynamic loads

(a)   Original Structure   (b)   Idealized Structure
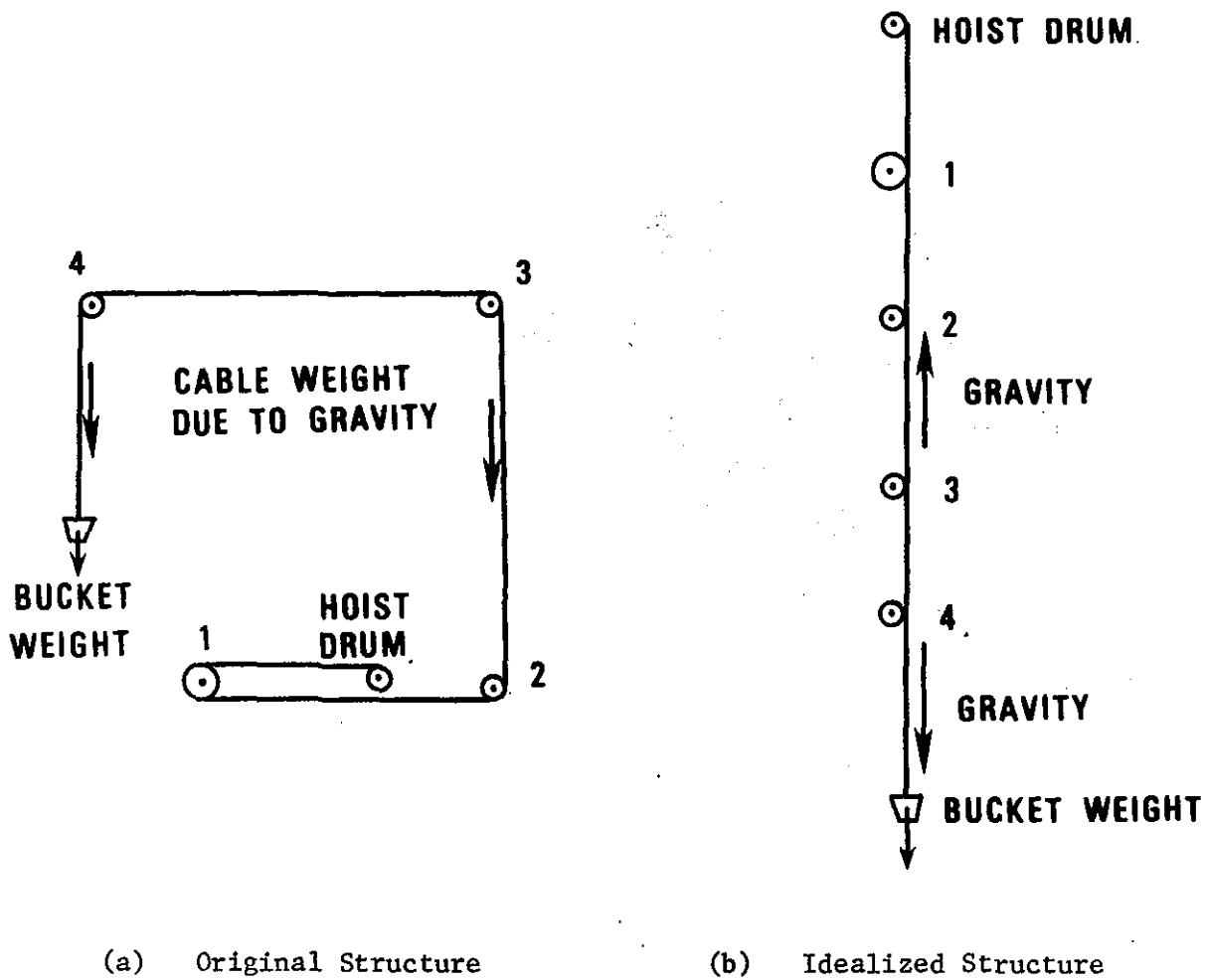
Figure 2.5   Idealization of hoisting cable as a
one-dimensional system

(a)   Original Structure   (b)   Idealized Structure
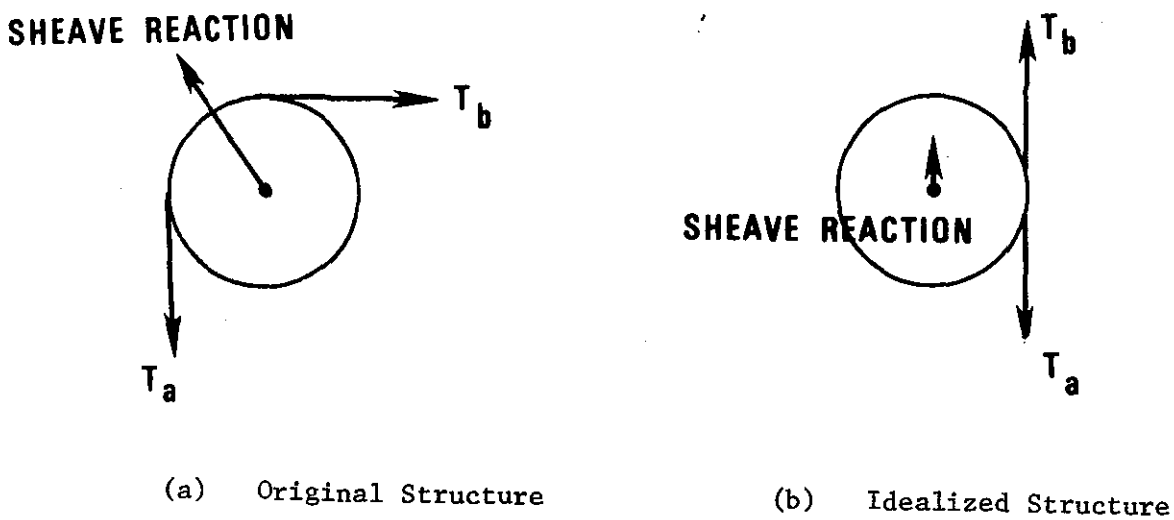
Figure 2.6   Sheave reactions of actual and
idealized systems

SLIDE PLATE ASSEMBLY

INSIDE SHEAVE

CATHEAD BEAM

G

PULLEY

COUNTERSTATIC
LINE

OUTSIDE
SHEAVE

CATHEAD
LEGS

K

HOIST
LINE

JUMP-
FORM
BEAMS

CHORD OF
STATIC LINE

WF
BEAM

UPPER
DIAGONAL

TOP OF
LIFT 28

LOWER
DIAGONAL

TOP OF
LIFT 27

STATIC
LINE

JACKING
FRAMES

(INSIDE)

(OUTSIDE)

SKID
BOARD

TOP OF
LIFT 26

ROLLERS

Scale: 5 ft

1 m

B

B₁ (GROUND ANCHOR BEFORE SHIFT TO B)
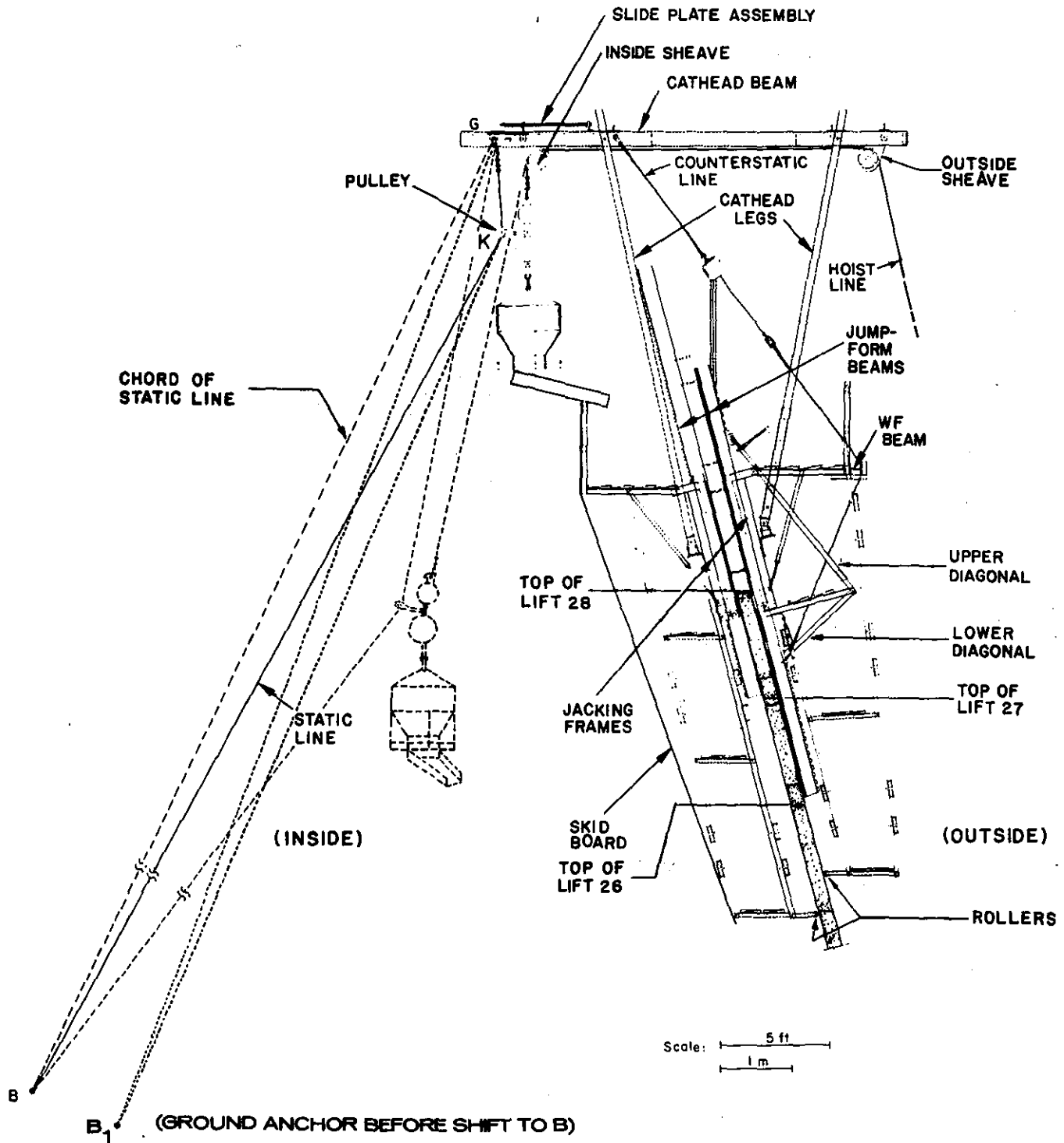
Figure 2.7   Detail of static and hoist lines

29
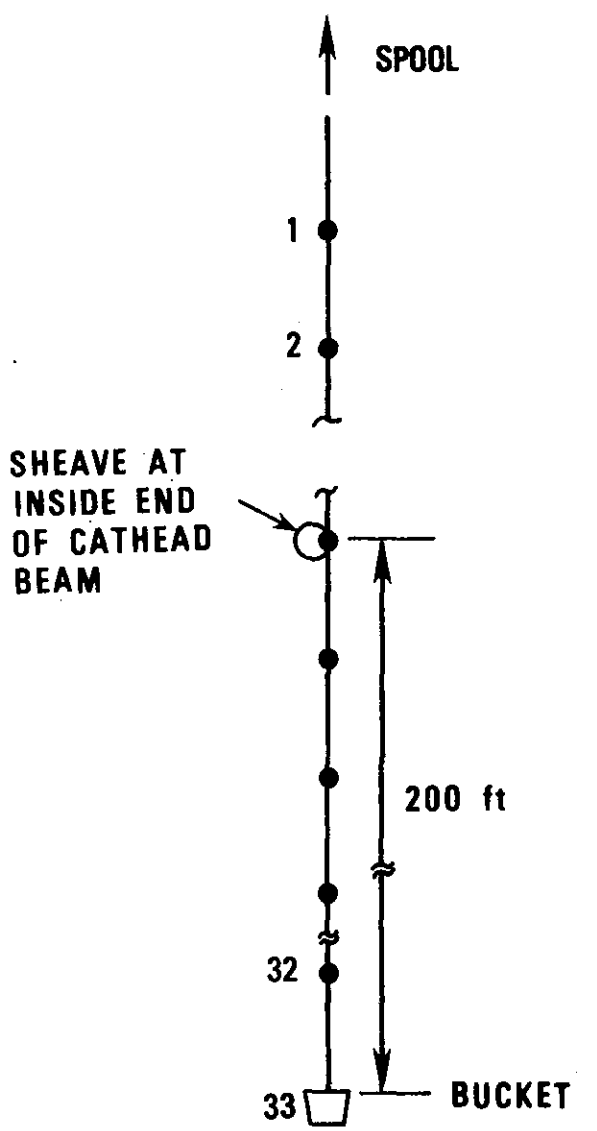
(a)   Initial Configuration
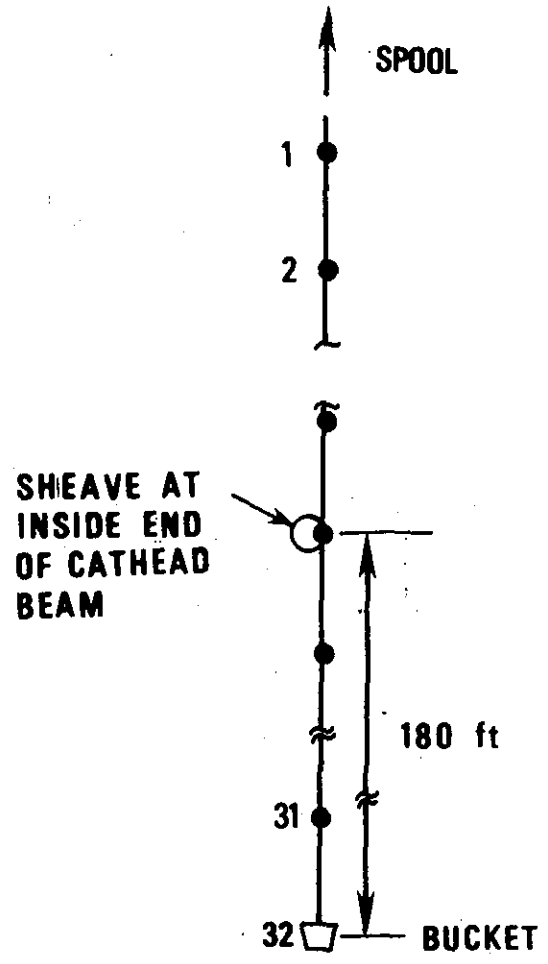
(b)   Renumbered Configuration
after Eliminating One Node

Figure 2.8   Node renumbering during analysis

30

EQUIVALENT
LINEAR
VELOCITY
OF DRUM
(fps)

0

2 TO 8 SEC   TIME
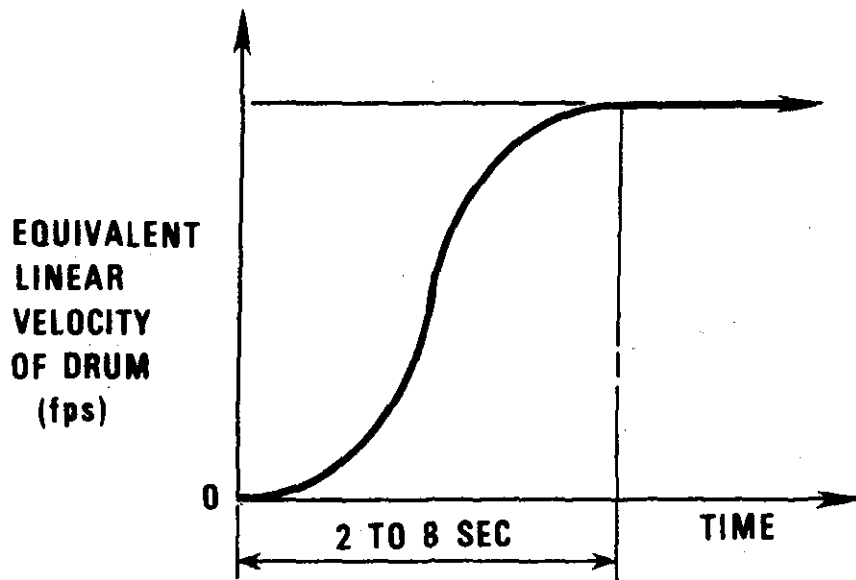
1.0 fps = 0.305 m/s

Figure 2.9   Assumed velocity profile,
              load case A - initially taut cable

10

EQUIVALENT
LINEAR
VELOCITY
OF DRUM
(fps)

4

0

2 TO 8 SEC   TIME
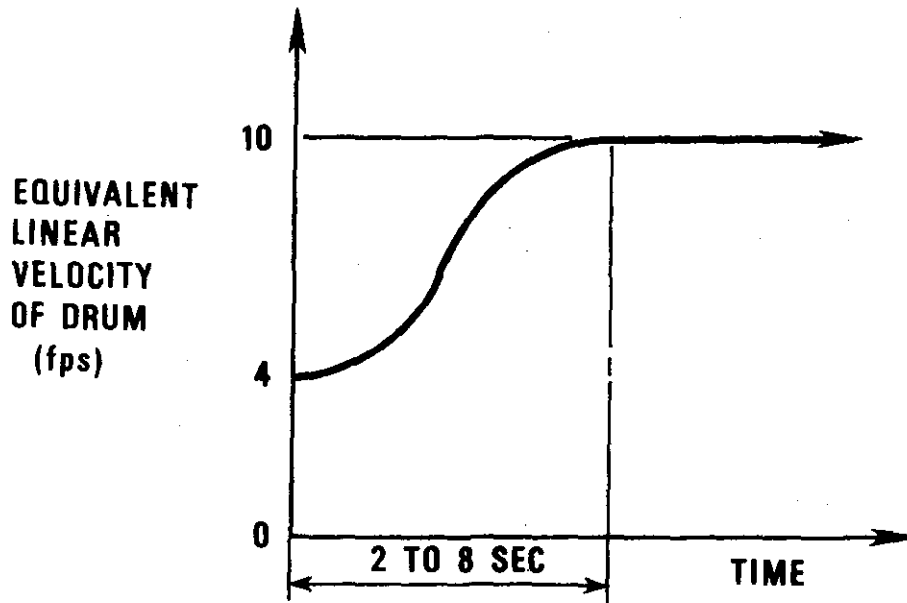
1.0 fps = 0.305 m/s

Figure 2.10   Assumed velocity profile,
              load case B - initially slack cable

31
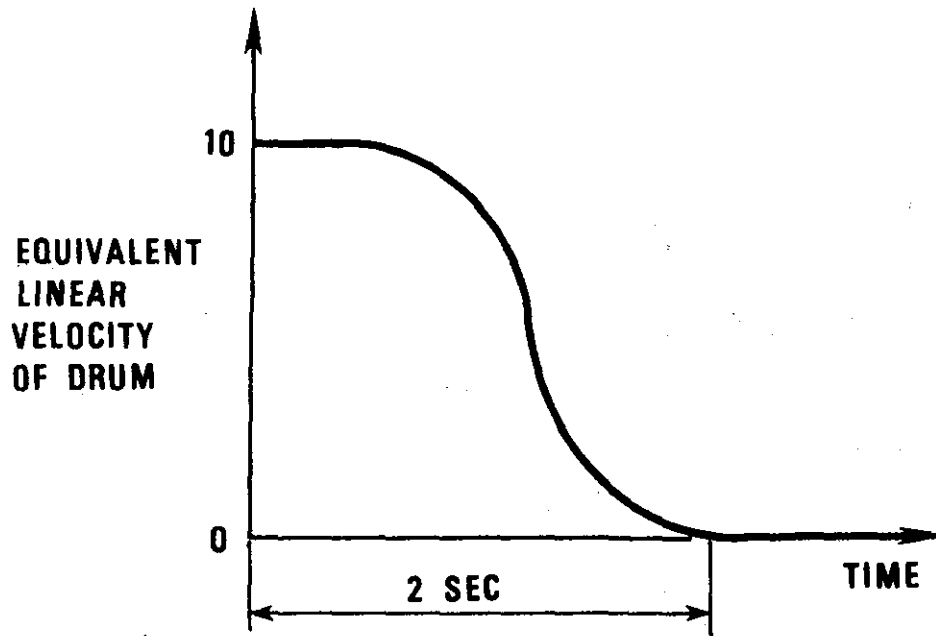
1.0 fps = 0.305 m/s

Figure 2.11   Assumed velocity profile,
load case C – braking force
applied to taut cable
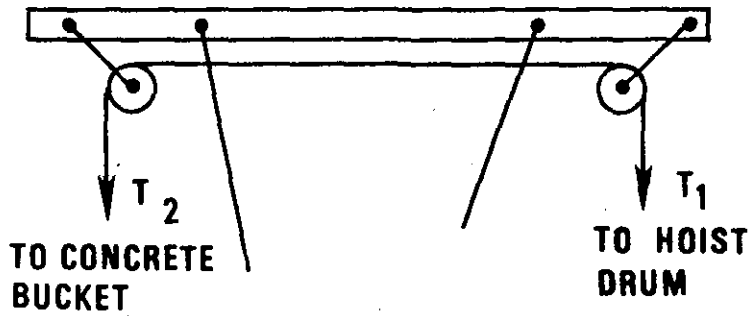
Figure 2.12   Unbalanced forces on cathead beam
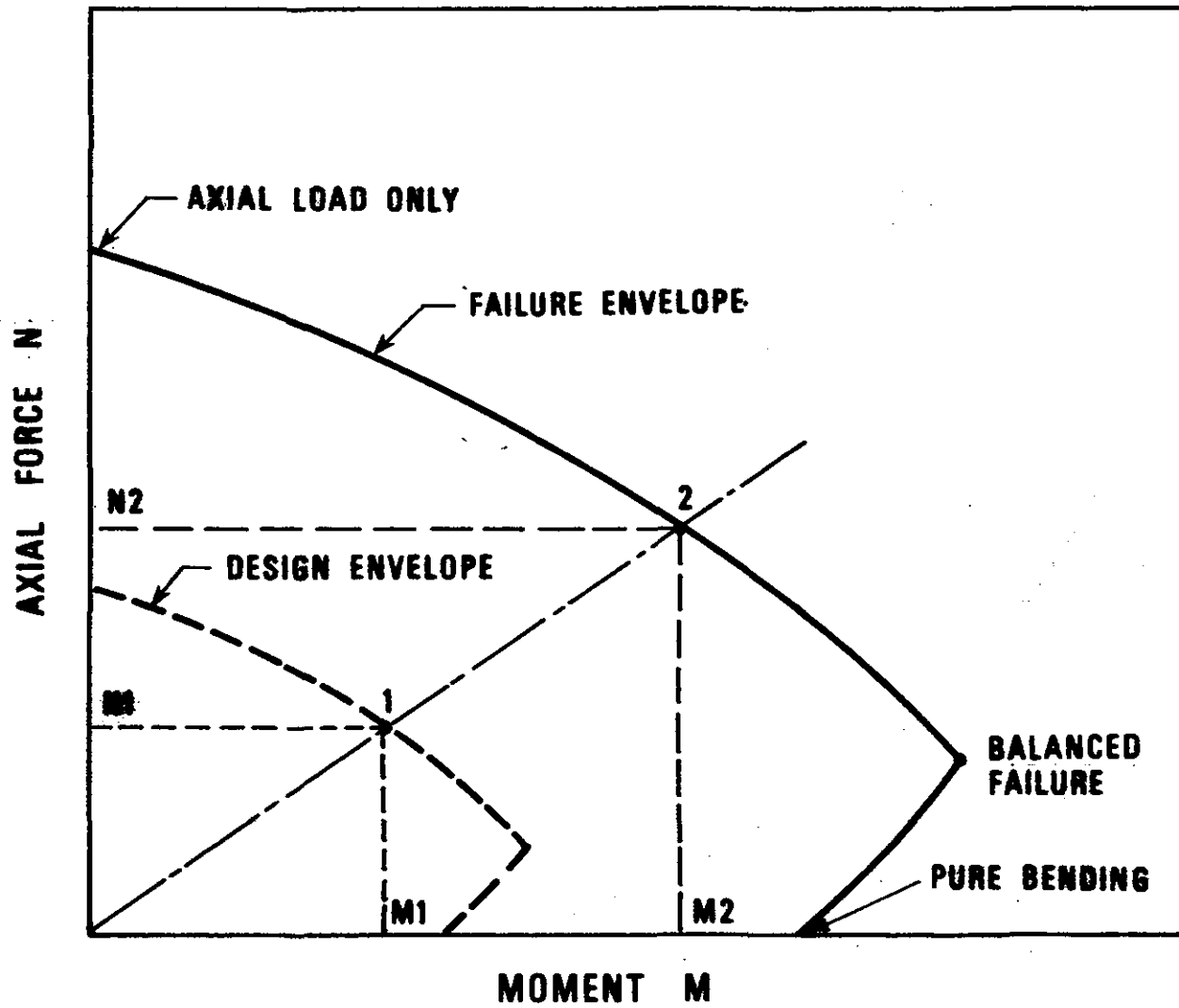
Figure 3.1   Flexure – compression interaction diagram
for concrete beam-columns
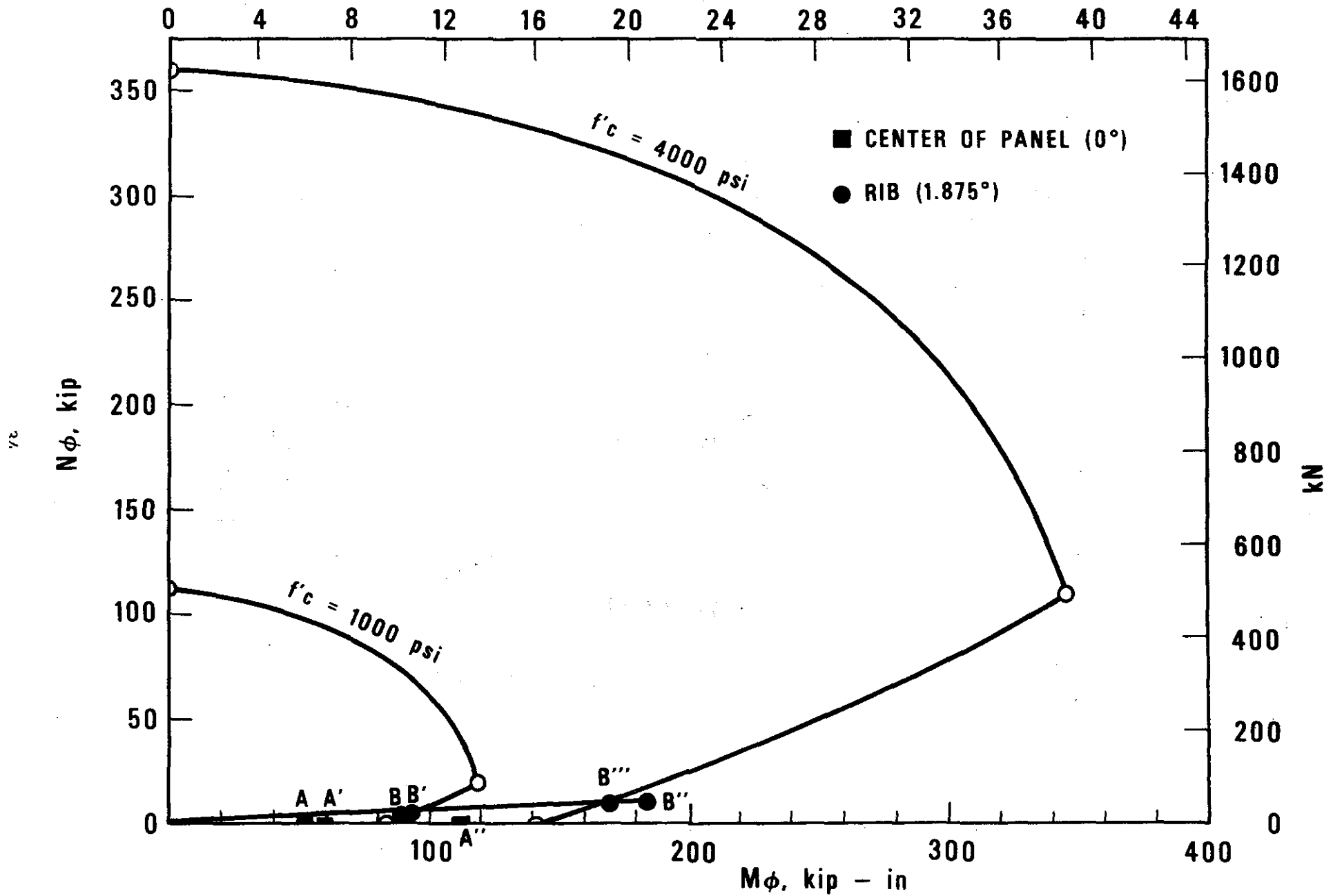
Figure 3.2 Comparison of meridional stress resultants at locations
A and B with the ultimate capacity of concrete section
for f'_c = 1000 and 4000 psi (6.9 and 27.6 MPa)
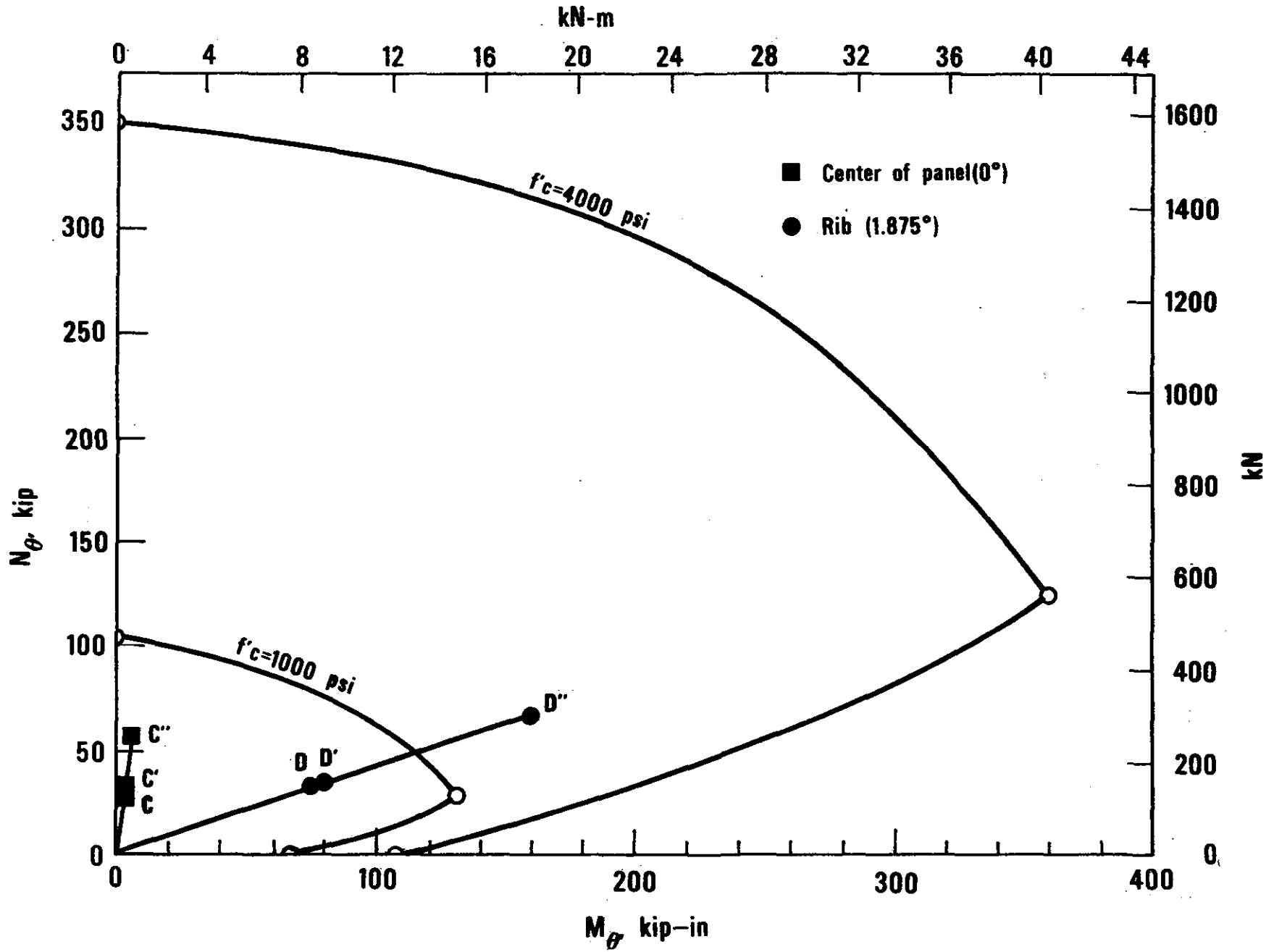
Figure 3.3   Comparison of hoop stress resultants at locations
C and D with the ultimate capacity of concrete section
for f'_c = 1000 and 4000 psi (6.9 and 27.6 MPa)

Cathead gantry

Jumpform beams

Stiffback channel

Level 1

Stiffback channel

29

Jacking frame

Jacking frame

Level 2

28

Scaffold

Anchor bolt

Level 3

27

Jumpform beam not bolted to the shell at this location

Steel skidboard

Level 4
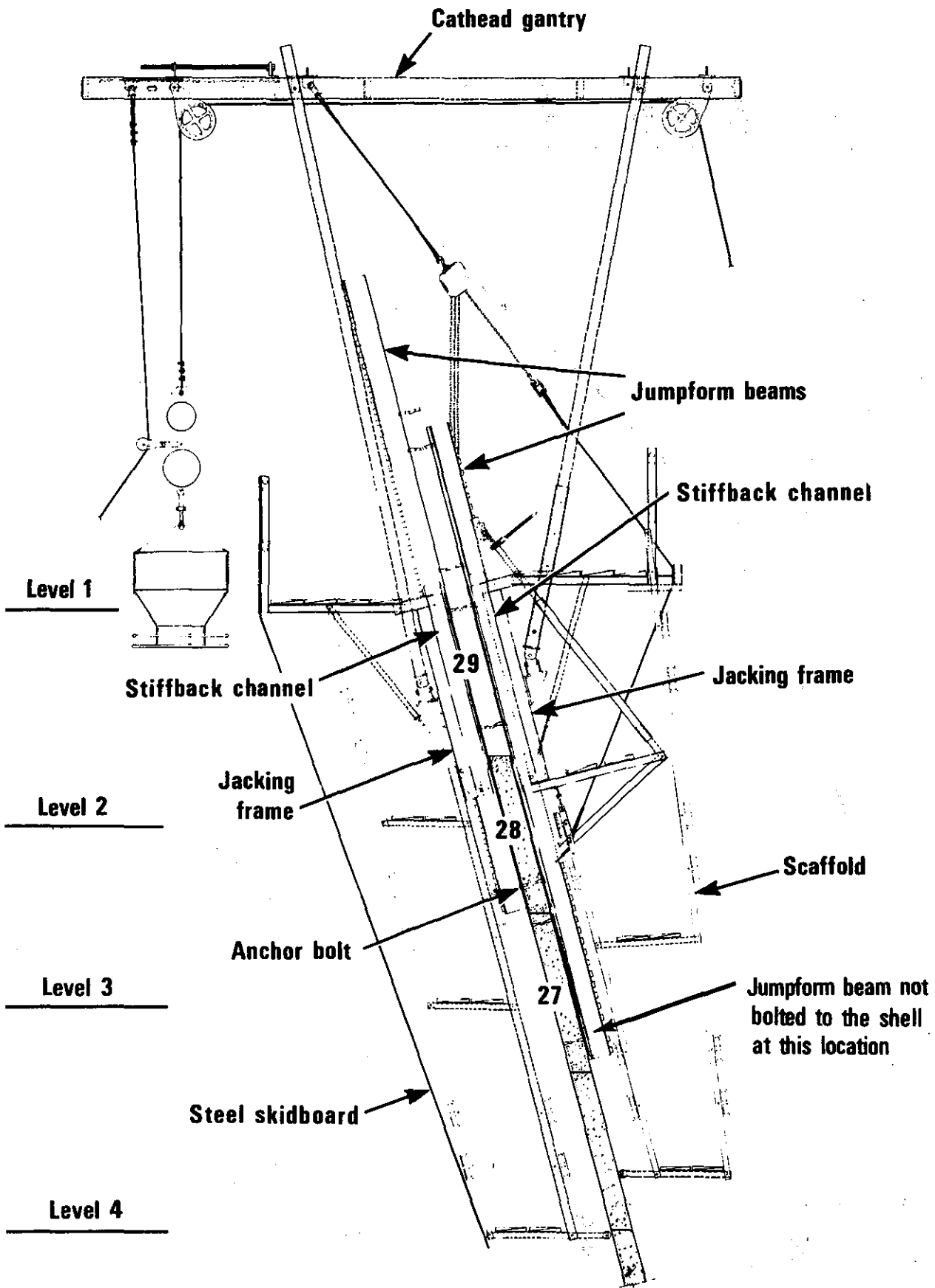
Figure 4.1   Cross section through formwork and scaffolding system

36
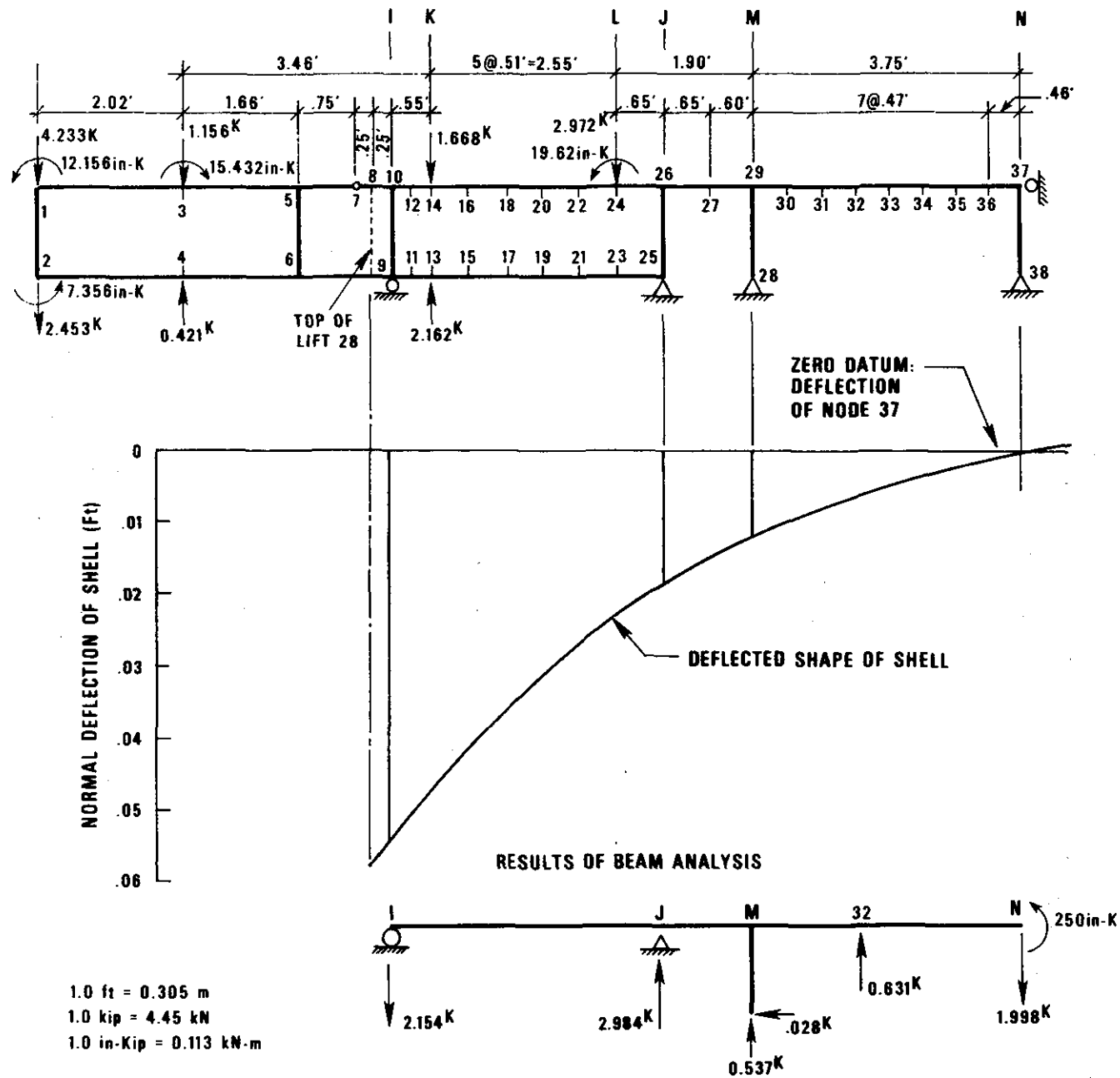
Figure 4.4   Analytical model of jumpform beam-anchorage assembly
and results

37
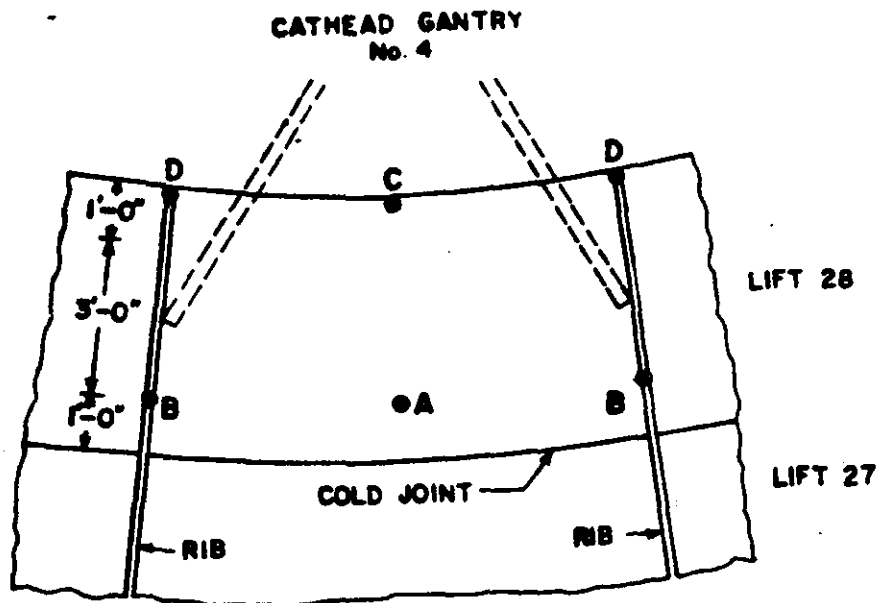
Figure 4.2 Location of maximum hoop and meridional stress resultants
in lift 28 (points C,D and A,B, respectively)
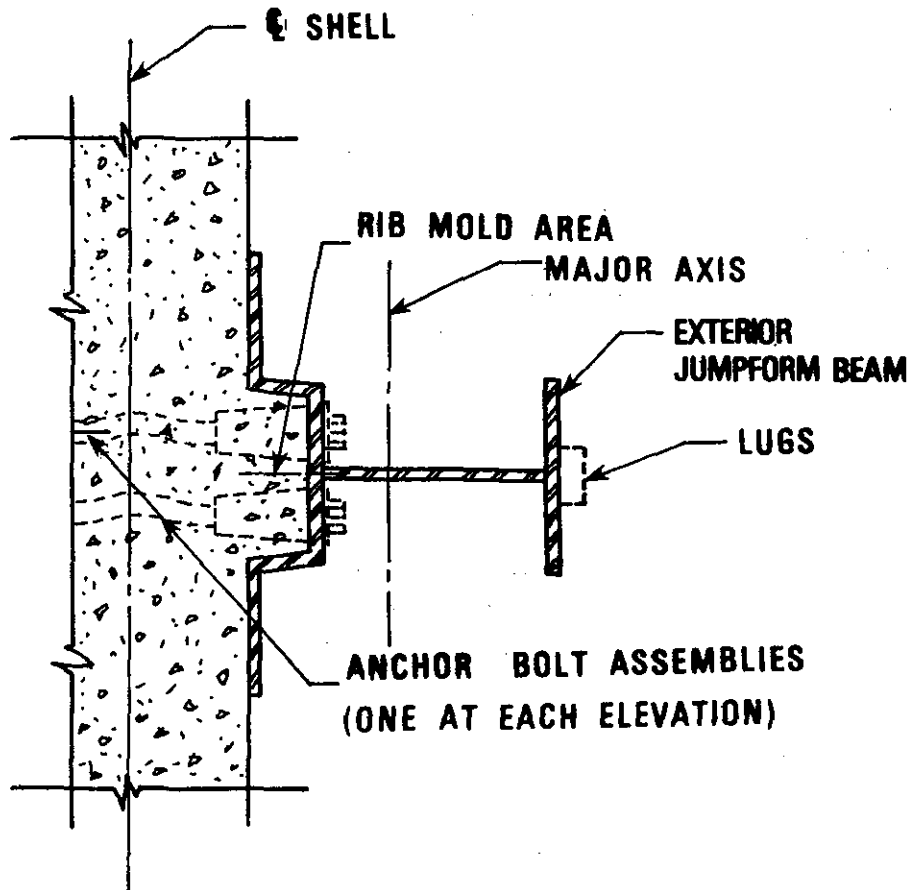
Figure 4.3   Sectional configuration at the interface
of exterior jumpform beam and concrete shell
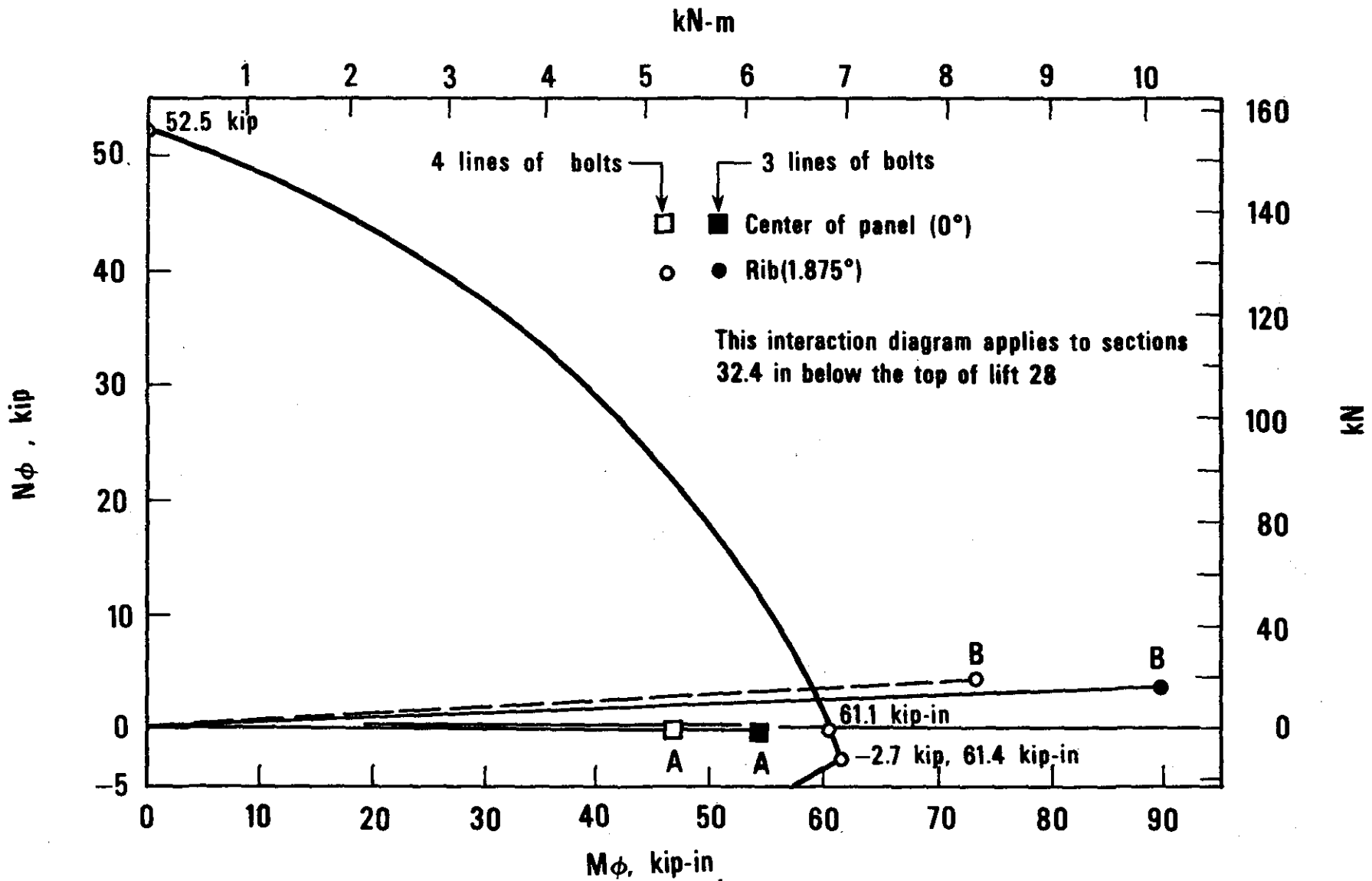
Figure 4.5   Comparison of meridional stress resultants at locations
A and B with capacity of concrete section for f'_c = 220
psi (1.52 MPa)
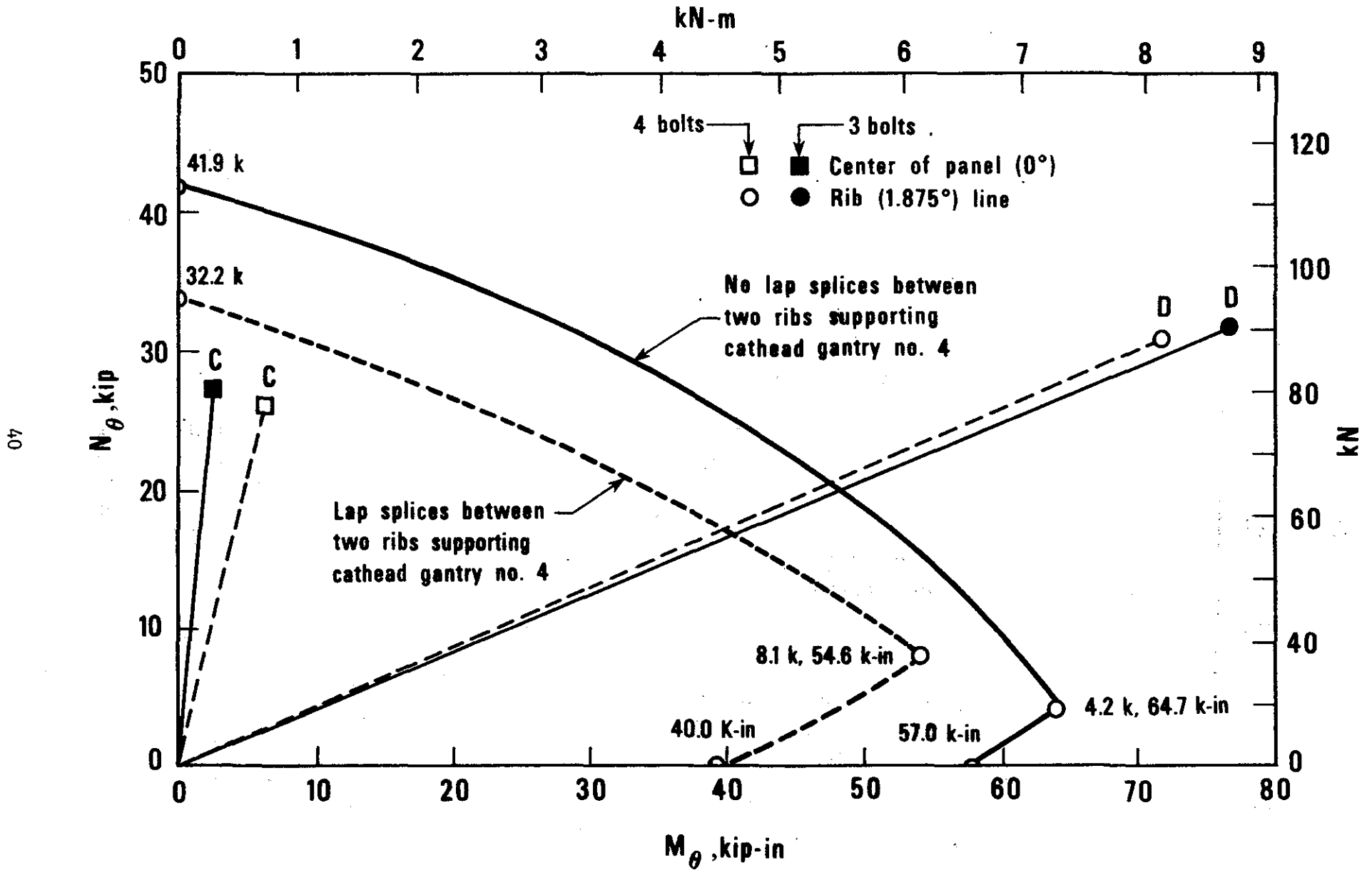
Figure 4.6   Comparison of hoop stress resultants at locations
A and B with capacity of the concrete section for
f'_c = 220 psi (1.52 MPa)

BEAM OF CATHEAD 4

HOISTLINE

196.28'

192.38'

STATIC LINE

38.94'
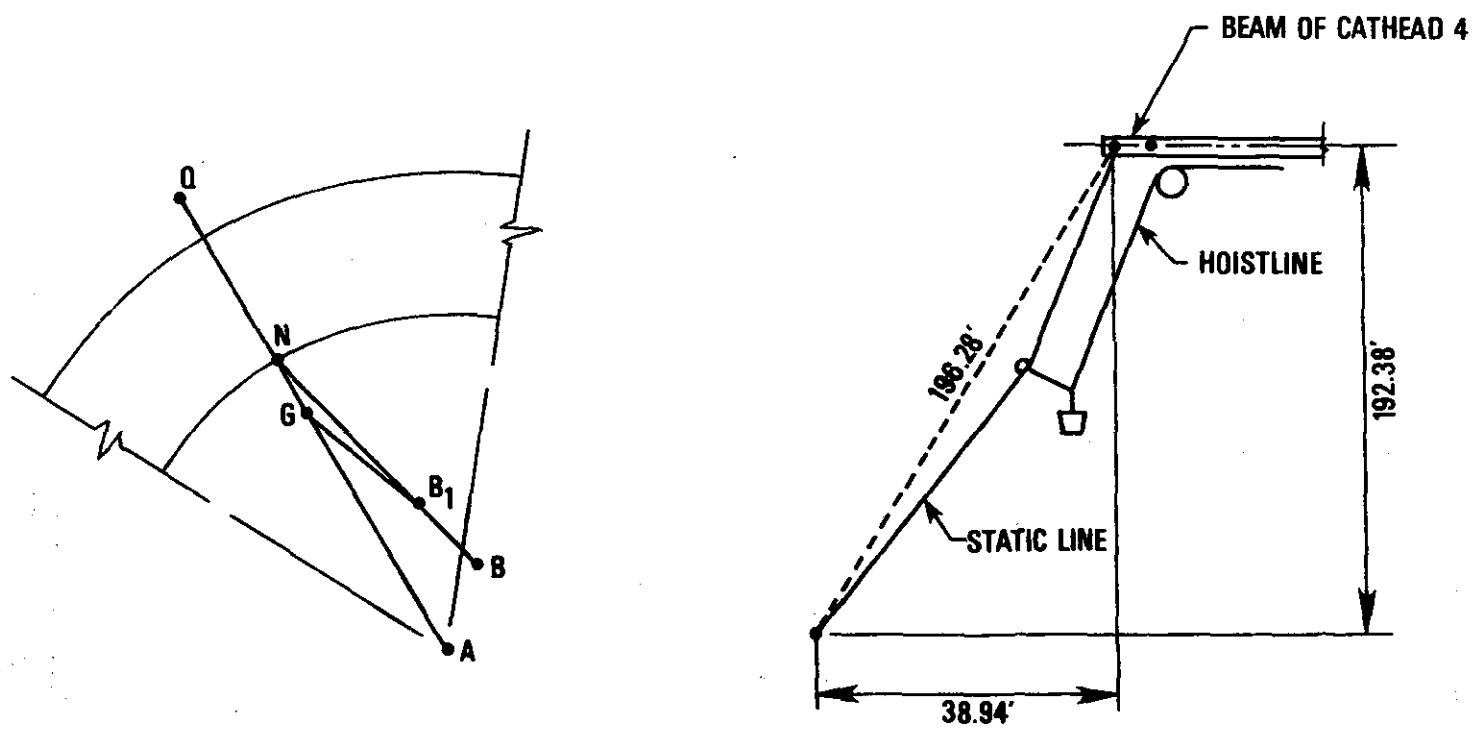
PLAN

ELEVATION

SPACE COORDINATES OF (ft):

	B_1	B
	N 976.76	N 927.94
	E 963.11	E 1022.66
	EL 97.81	EL 104.92

(SUPPLEMENTARY INFORMATION FIG. 6.2, REF 1)

1 ft = 0.305 m

Figure 5.1   Layout of static line of cathead no. 4
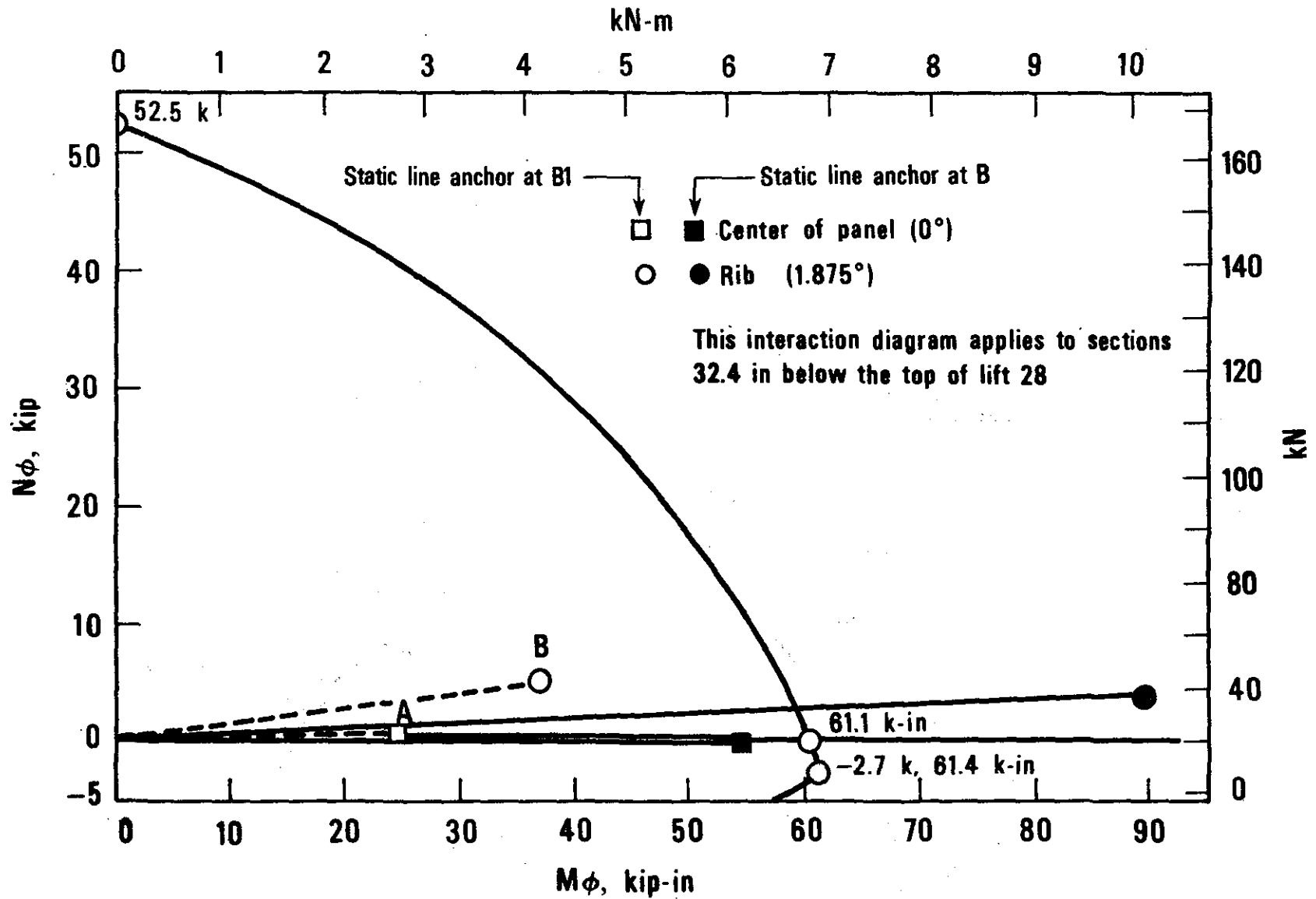
Figure 5.2   Sectional capacity of concrete for f'_c = 220 psi (1.52 MPa) stress resultants at locations A and B in the shell

Figure 5.3   Section capacity of concrete for f'_c = 220 psi
(1.52 MPa) vs. hoop stress resultants at locations
C and D in the shell